Journal of Materials Chemistry B

ROYAL SOCIETY OF CHEMISTRY

REVIEW

View Article Online
View Journal | View Issue

Cite this: J. Mater. Chem. B, 2021, 9, 594

Chitosan-based smart hybrid materials: a physico-chemical perspective†

Giuseppe Cavallaro,[a] Samantha Micciulla,*[b] Leonardo Chiappisi*[b] and Giuseppe Lazzara*[a]

Chitosan is one of the most studied cationic polysaccharides. Due to its unique characteristics of being water soluble, biocompatible, biodegradable, and non-toxic, this macromolecule is highly attractive for a broad range of applications. In addition, its complex behavior and the number of ways it interacts with different components in a system result in an astonishing variety of chitosan-based materials. Herein, we present recent advances in the field of chitosan-based materials from a physico-chemical perspective, with focus on aqueous mixtures with oppositely charged colloids, chitosan-based thin films, and nanocomposite systems. In this review, we focus our attention on the physico-chemical properties of chitosan-based materials, including solubility, mechanical resistance, barrier properties, and thermal behaviour, and provide a link to the chemical peculiarities of chitosan, such as its intrinsic low solubility, high rigidity, large charge separation, and strong tendency to form intra- and inter-molecular hydrogen bonds.

Received 31st July 2020,
Accepted 16th November 2020

DOI: 10.1039/d0tb01865a

rsc.li/materials-b

Introduction

Chitosan is commonly obtained from the deacetylation of chitin, the second most abundant natural polymer on earth after cellulose.[1] The primary sources of chitin are crustaceans such as crabs, shrimps and lobsters, which are highly abundant waste products from the food, beverage and canning industries.[2,3] The backbone of chitosan is very similar to that

[a] Dipartimento di Fisica e Chimica, Università degli Studi di Palermo, Viale delle Scienze pad 17, 90128 Palermo, Italy. E-mail: giuseppe.lazzara@unipa.it
[b] Institut Max von Laue – Paul Langevin, 71 avenue des Martyrs, 38042 Grenoble, France. E-mail: micciulla@ill.eu, chiappisil@ill.eu

† Electronic supplementary information (ESI) available. See DOI: 10.1039/d0tb01865a

Giuseppe Cavallaro

Giuseppe Cavallaro is an assistant professor at the Department of Physics and Chemistry, University of Palermo, Italy. He was a Research Associate at the Institute of Micromanifacturing, Lousiana Tech University, (USA) and Institut fur Chemie, Technische Universitat Berlin (Germany). His research activities focus on nano-clays and polymer/nanoparticle interactions. He is the author of more than 75 publications in peer-reviewed international journals.

Samantha Micciulla

Samantha Micciulla is a research and instrument scientist at the Institut Laue-Langevin in Grenoble, France. In 2016, she received her PhD degree in Applied Physical Chemistry at the Technische Universität Berlin, Germany, and then she was a Post-Doc fellow at the Max-Planck Institut for Colloid and Interface Science in Potsdam, Germany. With a background in polymer science and physical chemistry of soft matter at interfaces, she has been in charge of projects on the design of multi-functional responsive coatings based on polymers, including hybrid organic–inorganic composites, and of technical strategies for the investigation of separation-dependent structures of interacting soft interfaces.

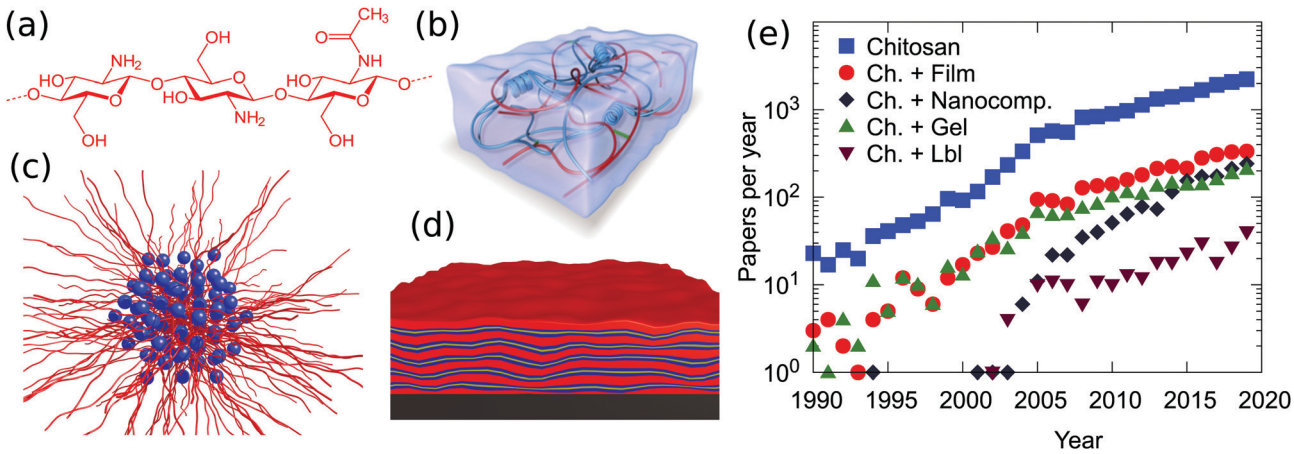

Fig. 1 (a) Chemical structure of chitosan and schematic representations of (b) a hybrid hydrogel from ref. 12, (c) chitosan/surfactant complexes, (d) chitosan-based layered coatings and (e) the number of publications per year on chitosan based materials. Data are from Scopus and they were obtained on 1 June 2020 using as searching string TITLE-ABS-KEY ("Chitosan" and "material") or ("Chitosan" and "material" and "film"), ("Chitosan" and "material" and "gel"), ("Chitosan" and "material" and "LbL") or ("Chitosan" and "material" and "nanocomposite").

of cellulose, with the hydroxyl group at the C2 position replaced by either an amino or an acetylamino group. Thus, chitosan is a copolymer consisting of *N*-acetyl-2-amino-2-deoxy-D-glucopyranose and 2-amino-2-deoxy-D-glucopyranose, where the two types of repeating units are linked by (1 → 4)-β-glycosidic bonds. The chemical structure of chitosan is shown in Fig. 1a. It is available within a large range of molecular weights and degrees of deacetylation. These two parameters largely alter the physico-chemical properties of the biopolymer and therefore a variety of specific applications can be considered based on viscosity, biological activity, biodegradability, wettability, colloidal stability and pH responsive features. Chitosan is readily soluble in dilute acidic solutions below pH 6.0 due to the protonation of the amine groups (a pK_a value of 6.3). Furthermore, it has gel, fiber and film forming properties. From the biological point of view it shows antimicrobial activity and good compatibility with living tissue.

Chitosan exhibits a combination of physico-chemical features which make this polymer a fundamental component in materials science. With the exception of cationically modified cellulose, it is one of the very few cationic biopolymers available. The saccharidic backbone provides this macromolecule with three fundamental peculiarities, not found in other polymers: (i) a high intrinsic rigidity, with reports of persistence lengths which vary between 5 and 30 nm;[4,5] (ii) a relatively large spacing between the charges, with a maximum of 1 change per 5 Å in the case of a fully deacetylated polymer. The actual value is in reality much closer to the Bjerrum length in water of 7.1 Å, *i.e.*, the distance at which the magnitude between electrostatic interactions approaches the thermal energy. The consequence of the large separation, in combination with the high intrinsic rigidity, is the fact that the polymer conformation in solution is less affected by the type and concentration of counterions or by the binding to oppositely charged colloids compared to

Leonardo Chiappisi

Leonardo Chiappisi received his PhD in 2015 in Physical Chemistry from the Technische Universität Berlin. In his PhD thesis, he investigated chitosan-based responsive assemblies with oppositely charged surfactants. Since 2015 he has been working at the Institut Laue-Langevin, the European flagship for neutron science. His research activity is focussed on the investigation of complex colloidal systems, both in bulk and at interfaces.

Giuseppe Lazzara

Giuseppe Lazzara has been an associate professor at the Department of Physics and Chemistry, University of Palermo, Italy, since 2015. He received his PhD degree in Chemistry in 2007. He was a Postdoc fellow at the Chemistry Department, Lund University (Sweden). He is involved in several projects on halloysite clay nanotubes for drug delivery and materials for the conservation of cultural heritage. Lazzara has more than 150 publications in peer-reviewed international journals, an edited book and 2 patents in the field of nanomaterials for cultural heritage.

high charge density, flexible polymers. (iii) A high tendency of forming intra- and inter-molecular hydrogen bonds. Such hydrogen bonds increase, on one hand, the rigidity of the polymer backbone and are, on the other hand, at the origin of the very low tendency of mixing between polysaccharides and other polymers.

Chitosan-based materials have been reviewed in different fields, from molecular separation to food packaging films, from artificial skin to bone substitutes and water treatment.[3,6,7] Most of the reviews are focused on a given application of the chitosan-based materials[6–10] or in some other cases they explore a wide range of biopolymers, including chitosan, for some specific applications.[11] How these and further peculiarities affect the properties of soft, chitosan hybrid compounds in aqueous environments, in thin films, and in nanocomposite systems, schematically represented in Fig. 1b–d, is discussed hereafter.

It is also useful to recall that chitin, the precursor of chitosan and the main structural component of the exoskeleton of crustaceans, is, by design, a very poorly soluble polymer. This intrinsic property is retained in chitosan, the solubility of which in acidic aqueous environment is simply given by the translational entropy of the counterions. In other terms, as soon as the soluble counterions, often acetate ones, are exchanged with much less soluble macroions such as polymers, micelles, or clay particles, the formation of an insoluble complex is observed. We find this general tendency throughout the physico-chemistry of chitosan-based systems, and, in the course of this review, we will highlight how this phenomenon is exploited and which strategies were developed to increase the solubility.

As illustrated in Fig. 1e, chitosan is highly employed in materials science. Film and gel formulations are the most traditional investigated materials, since 2005 nanocomposites have been growing. Until now, less explored but promising, is the possibility to prepare a layer-by-layer system using chitosan as the cationic biopolymer. The observed trends suggest that although the applications of this polymer have been established, some properties, such as mechanical strength, thermal stability, low water content and gas barrier properties, were not good enough to meet this wide range of applications. The preparation of hybrid materials based on chitosan, with both organic and/or inorganic fillers, overcomes some intrinsic limitations and opportunely tunes the physico/chemical properties of the material.

Soft materials in aqueous media

The above-mentioned properties of chitosan make this polymer a unique building block in the field of colloidal chemistry. Accordingly, substantial efforts have been made to characterize chitosan hydrogels or complex mixtures of chitosan with surfactants, polymers, emulsions, *etc.*

Chitosan/surfactant systems

Mixtures of chitosan and surfactants have been a matter of intensive studies.[13–15] Given its cationic nature, particular attention has been paid to mixtures of chitosan with oppositely charged anionic surfactants. It can be safely stated that chitosan forms insoluble complexes with strongly ionic surfactants over a wide range of concentrations and mixing ratios,[13,16–18] with the formation of insoluble complexes even at very low surfactant concentrations (mM) and large polymer excess.[15] A clear explanation of this extremely pronounced low solubility has not been found yet, and the experimental results point towards a kinetically trapped state and highly cooperative binding. The high tendency to form water-insoluble complexes has been exploited for the preparation of beads,[13,19] the size of which can be controlled by the preparation method and varies between a few hundred nanometers and a few centimeters. The thickness of the bead wall shows an initial growth with the square root of time, indicating a diffusion controlled process.[13] Such beads are highly promising for pollutant recovery applications.[19,20] Few studies have been focused on the interaction of chitosan with fatty acids.[21–24] Due to the fact that chitosan is soluble in a slightly acidic medium, while long and medium chain fatty acids are solubilized in alkaline conditions, soluble mixtures are found only when chitosan is mixed with short chain carboxylic acids, such as formic, acetic, butyric and valeric acid.[21,25] Due to the short alkyl chain, the interactions in these systems are purely electrostatic.[21] As soon as the alkyl chain is long enough, lateral, hydrophobic interactions favor the spontaneous formation of micelles, and a much more complex behavior in mixtures with chitosan is observed. This is the case, for instance, of mixtures with undecylenic acid, which exhibit the formation of supramolecular aggregates with a typical size of a few hundred nanometers.[26] Mixtures of chitosan with long chain acids, such as oleic, linoleic, palmitic, and stearic acid, have also been studied,[22,27] despite their low solubility, as mentioned before. A schematic representation of the structures formed in carboxylic acid/chitosan mixed systems is provided in Fig. 2. However, water soluble complexes can be obtained when chitosan oligosaccharides, which are soluble also in alkaline conditions, are used. An example is mixtures of chitosan oligosaccharide with oleic acid vesicles.[28,29] The coating by chitosan decreased the fluidity of the membrane and increased the stability of the liposomes towards shear and flow stresses.[28]

The strong limitation found for the incompatible difference in solubilities of chitosan and fatty acids is overcome when the fatty acids are chemically modified to include an oligoethylene oxide block between the aliphatic chain and the carboxylic acid termination. So-called alkyl ether carboxylates were shown to co-assemble with chitosan in a broad variety of structures which are highly responsive to external stimuli.[30–34] In particular, depending on the solution acidity and the molecular architecture of the surfactant, multilayer vesicles or compact aggregates embedding small surfactant micelles are obtained.[14,31,34] To the best of our knowledge, these surfactant/chitosan systems show the largest structural variety with an exquisite response to pH variations. The large structural variety derives from the high control over the surfactant packing parameter, depending on pH and the ratio between the alkyl

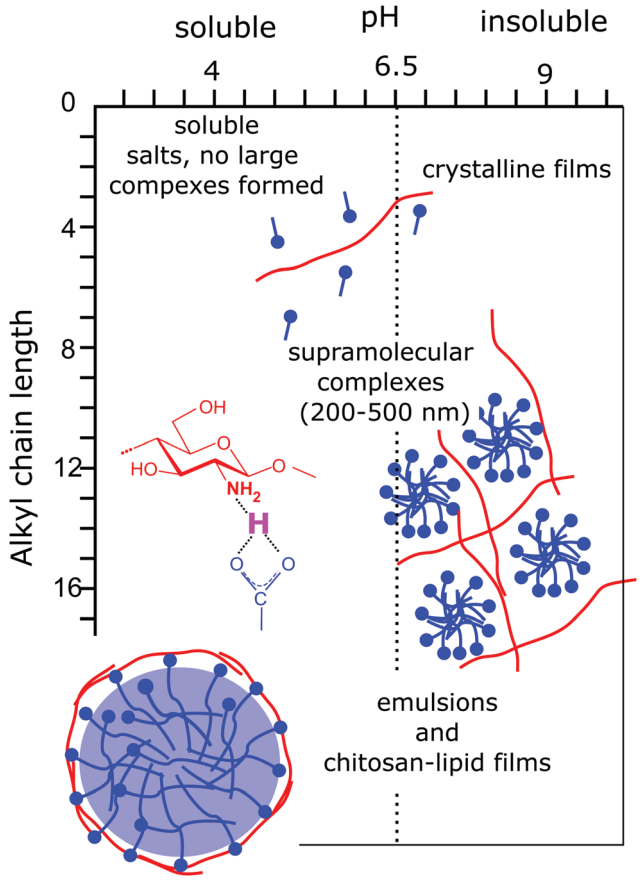

Fig. 2 Schematic representation of structures and the interaction mechanism found in chitosan/carboxylic acids as a function of the acidity of the solution and of the length of the alkyl chain. Insets present the structures observed in the mixtures and provide an insight into the ionic hydrogen bond formed between the carboxylic acid termination and the amine moiety of chitosan. Adapted from ref. 15, copyright 2020, with permission from Elsevier.

chain and the size of the oligo ethylene oxide block. The strong response to even very little changes in solution acidity derives from the very specific ionic hydrogen bond between the carboxylic surfactant termination and the amine moiety of the macromolecule with an estimated strength of 10 k_BT.[32,35] In contrast to generic electrostatic interactions, the ionic hydrogen bridges are extremely localized and their strength is strongly dependent on pH. The peculiarity of this bond is probably also at the origin of the very unique observation of chitosan–fatty acid mixtures becoming less soluble upon the addition of a nonionic surfactant.[32] Finally, the strong structural response of these systems towards mild variations in pH can be exploited for the formulation of environmentally friendly delivery and recovery systems.[34]

Chitosan-based polyelectrolyte complexes

The formation of supramolecular complexes in mixtures with anionic polyelectrolytes has been extensively studied, and we address the readers to some extensive reviews.[36,37] As indicated in the introduction, chitosan is an intrinsically insoluble polymer, and its solubility is provided by the counterion cloud. In mixtures with oppositely charged polyelectrolytes, these many, soluble counterions are exchanged with an ionic macroion. Accordingly, the most common finding is that an insoluble coacervate is formed. This condition has motivated the establishment of various strategies to prepare more water-soluble systems, such as dispersed colloidal complexes or hydrogels. The formation of complexes can also be exploited for the formation of thin films, which are discussed in the next section of this review. A schematic description of the different typologies of chitosan-based polyelectrolyte complexes is given in Fig. 3.

Mixtures of chitosan with virtually every other available polyanion were investigated. However, particular attention has been paid to complexes with polynucleotides, such as DNA[38–42] or RNA,[43–46] with anionic polysaccharides, such as alginate,[9,47–50] hyaluronic acid,[51,52] dextran sulfate,[53,54] or synthetic polyelectrolytes, such as poly acrylic acid.[55–58]

The main objective of studying chitosan–polynucleotide mixtures is the understanding and improvement of gene delivery systems.[59,60] In this sense, it is essential to determine the factors affecting the affinity between chitosan and the polynucleotide, in order to be able to balance the stability of the complexes and the delivery efficiency. A complex with a too high binding constant cannot release the gene to the target cell. In contrast, a complex with a too low affinity is not able to transport the gene sequence to the target cell. In this sense, isothermal titration calorimetry provides valuable insights into the binding affinity of chitosan and DNA or RNA.[40,42,46] The binding is mainly due to the electrostatic interaction between the charged amine group of the polysaccharide and the phosphate unit of the nucleic base[41,42] and is therefore affected by the degree of acetylation and the degree of ionization of chitosan.

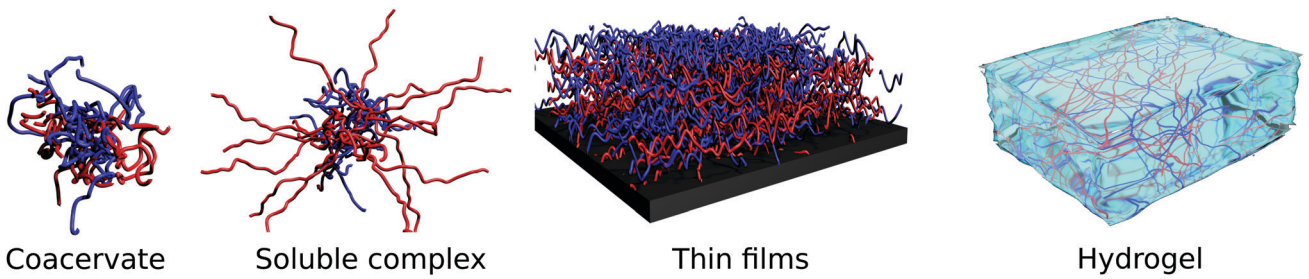

Fig. 3 Schematic representation of from left to right: complex coacervates, soluble complexes, solid supported thin films, and gellified systems obtained from mixtures of chitosan (in) and oppositely charged polyanions (in blue).

Given the biocompatible properties of anionic polysaccharides, such as alginate and hyaluronate, their complexes with chitosan have been extensively investigated, mainly as scaffolds for tissue engineering,[37,47,48] for drug delivery,[47,49] or for pollutant recovery,[9,50] to mention some of the most relevant applications. The properties of chitosan/alginate scaffolds can be further improved when a third component is added to the mixture, such as inorganic nanoparticles,[61–63] or using chemical cross-linking agents.[64,65] Similarly, chitosan/hyaluronic acid complexes are highly interesting in tissue engineering applications due to the combined flexible nature and antibacterial properties of such complexes. In particular, hydrogels can be formed *in situ* upon injection to the desired tissue due to the slow kinetics of gel formation.[66] When chitosan is mixed with dextran sulfate, a strongly charged polyion, the formation of capsules and beads is observed even in large excess of one of the components,[53,54] similarly as for mixtures of chitosan with sulfated surfactants described earlier.

Poly(acrylic acid) (PAA) is one of the most relevant synthetic weakly anionic polymers and complexes with chitosan were probed, mainly with the aim of designing pH-responsive delivery systems. The preparation of chitosan/PAA complexes follows two main routes: non-cross linked particles are prepared by mixing chitosan and PAA in different stoichiometries and experimental conditions;[55,56] cross-linked chitosan PAA particles are obtained when acrylic acid is polymerized in the presence of chitosan.[57]

Chitosan-based hydrogels

The challenge of preparing chitosan-based hydrogels lies in the fact that a significant amount of water needs to be retained in the system. Chitosan hydrogels are generally prepared by physical or chemical cross-linking of the polymer chains, keeping enough charges and/or hydrophilic moieties to guarantee sufficient hydration in the network. There are numerous protocols for the preparation of simple and hybrid chitosan hydrogels, which attract huge interest, in particular in the fields of biomedical applications[12,67,68] and wastewater treatment.[69]

Physically cross-linked simple hydrogels

Chitosan-based hydrogels are formed through physical or chemical cross-linking between the polymer chains. The simplest procedure consists in increasing the pH of the chitosan solution, thus strongly inducing the solubility of the polymer.[70,71] In practice, a concentrated solution of chitosan is brought into contact with an alkaline environment. The swelling of this precipitate/hydrogel is determined by the osmotic pressure of the counterions of the residual charges on the chitosan backbone. In particular, Enache *et al.* showed that the advancement of the gelation front can be adequately described with Fick's second law.[71] Moreover, different studies have reported that the chitosan hydrogel structure becomes more heterogeneous the larger the distance from the hydrogel surface.[70,71]

A different approach consists in using multivalent, negative ions to physically cross-link chitosan *via* electrostatic interactions. While tripolyphosphate is the most common anionic cross-linking agent,[72–75] examples of ionotropic gelation of chitosan by molybdate,[76] polyoxometalates,[77] sulfate,[78] citrate,[78] or phytate[12] have been also reported. A clear advantage of using tripolyphosphate as a cross-linking agent is the high mechanical stability of the obtained particles. For instance, it was shown that the mechanical strength of chitosan/tripolyphosphate gel beads is approximately ten times higher than that of the analogous beads prepared by cross-linking the polymer with sulfate and citrate.[78] Noteworthily, the chitosan/β-glycerophosphate system shows thermally induced gelation when the system is heated at 37 °C, thus being ideally suited for the preparation of injectable chitosan hydrogels.[79,80] A further interesting example is the formation of a hybrid chitosan–gelatin hydrogel, the mechanical properties of which are strongly enhanced upon the addition of phytate, a multivalent negatively charged ion, to the hydrogel[12] (as depicted in Fig. 4). This system provides an excellent example of how the physico-chemical properties of chitosan are linked to the hydrogel features. In fact, when chitosan is neutralized with sodium phytate, a rather dense precipitate is formed due to the high charge density and stiffness of the polysaccharide. In contrast, a well hydrated, elastic hydrogel is formed when chitosan is co-crosslinked with a flexible, hydrophilic, and loosely charged polymer such as gelatin. Finally, an important property found in chitosan hydrogels formed through ionic cross-linking with anionic polysaccharides is the self-healing capacity of these gels, which originates from the dynamic nature of the ionic cross-linking point.[61,81]

Chemically cross-linked simple hydrogels

Covalent cross-linking of chitosan is also performed in a routine fashion. In many cases, small molecules such as dialdehydes[82,83] or Genipin[84,85] are used. To improve the elasticity of the gel, polymeric cross-linking agents such as diepoxy polyethylene glycol or dicarboxylic acid polyethylene glycol are also employed.[86,87]

Hybrid hydrogels

To add new functionalities and to adapt the mechanical properties of the hydrogels to the desired needs, the formation of hybrid chitosan-based hydrogels has been extensively probed. The strong adhesive, anti-inflammatory, hemostatic, and bactericidal properties of chitosan make this polysaccharide an excellent candidate for a broad range of biomedical applications of hydrogels. We address the reader to some recent reviews on the topic.[6,67,68]

We have mentioned above the formation of hydrogels based on chitosan and hyaluronic acid for biomedical purposes.[52,66,88] To provide mechanical stability to these hydrogels, a covalent cross-linking between the two polysaccharides can be obtained *via* a Schiff base reaction. Chemical prefunctionalisation of chitosan with a *N*-succinyl group and of hyaluronic acid with an aldehyde one allows the reaction to occur *in situ* without the need for additional chemicals.[88] Similar cross-linking procedures are applied to other polysaccharide based hybrid hydrogels.[89,90] A plethora of different

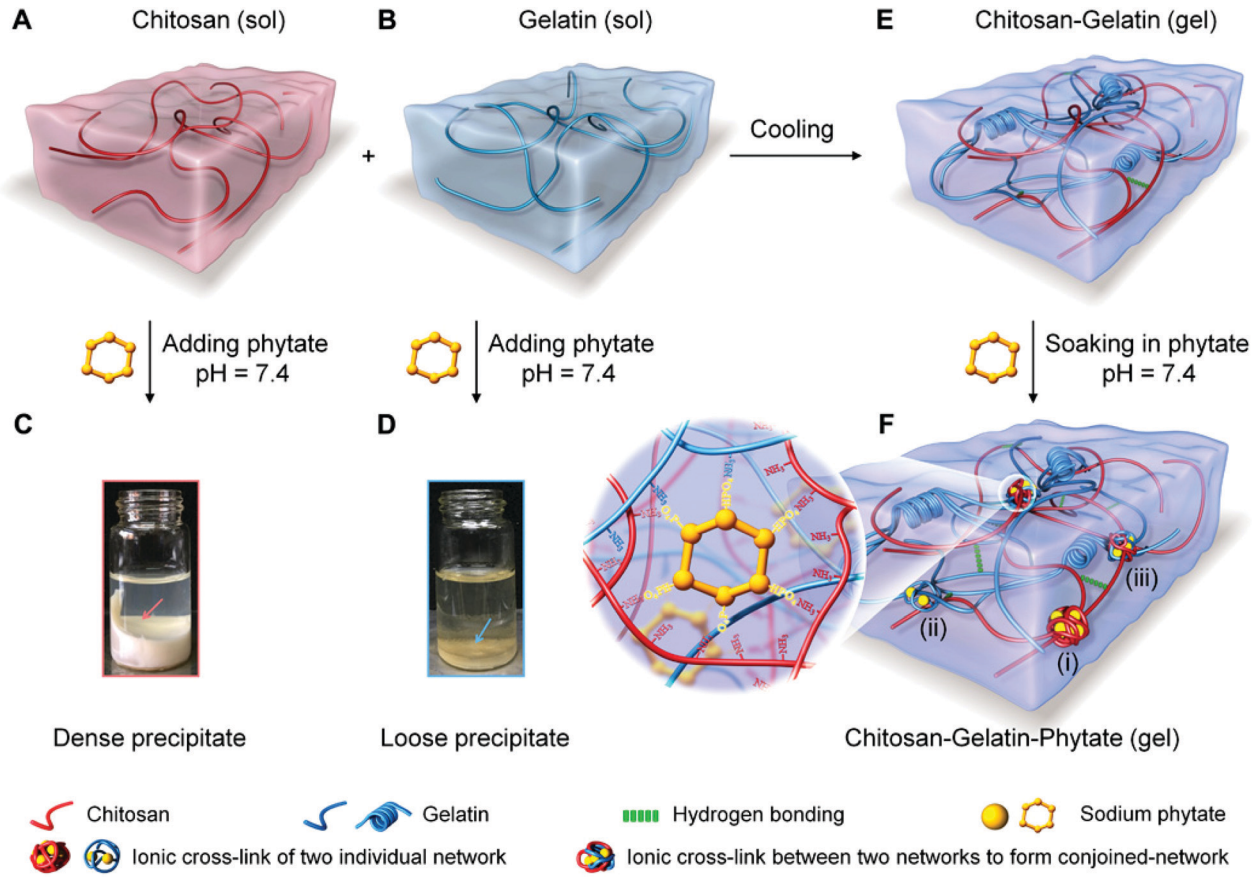

Fig. 4 Schematic representation of chitosan (A) and gelatin (B) solutions which form a composite hydrogel upon mixing and cooling (E). Optical photos of the dense precipitate formed by chitosan (C) and of the loose precipitate formed by gelatin (D) upon the addition of sodium phytate. The different degree of hydration of the precipitate is a direct consequence of the different charge density and stiffness of chitosan and gelatin. (F) Schematic representation of the chitosan, gelatin, phytate conjoined-network hydrogel. The inset illustrates the structure of the network consisting of physical bridging between the polymer chains cross-linked by multivalent counterions. The cross-bridging of the two networks allows a unique combination of high compressive modulus and toughness to be obtained. Reprinted with permission from ref. 12.

chemical modifications of chitosan to enable the chemical cross-linking within chitosan/polysaccharide networks is described in the literature[91,92] and the right choice must be dictated by the field of application, the nature of the components, and the desired physical properties of the resulting hydrogel. Of note are externally-triggered cross-linking reactions, *e.g.*, by photoirradiation.[93,94]

In summary, extensive work has been performed on the characterization of chitosan-based hydrogels and the understanding of the correlation between molecular properties (the degree of substitution, charge density, complex solubility, and the final gel characteristics). In particular, their use in the field of tissue engineering seems to be highly promising, given the 3D network structure of the gel and the tunable mechanical properties, associated with the strongly adhesive, anti-inflammatory, and anti-bacterial properties of chitosan.

Self-assembly of chitosan-based thin films

Besides hydrogels, polysaccharide assemblies in the form of thin films are very well suited for the design of functional coatings dedicated to biomedical and biotechnological purposes.[95–99] Among them, chitosan-based thin films have been widely applied for drug delivery systems,[100–102] antibacterial[103–106] and antifungal surfaces,[102,107,108] food protection and paper packaging,[109,110] as well as wound healing.[111,112] The broad range of applications is possible, thanks to the excellent biocompatibility, biodegradability, low toxicity and high availability of chitosan, as well as to the tunable film properties (structure, elasticity, porosity) by adjusting both molecular composition and assembly conditions.[13]

One of the most commonly employed strategies for the formation of chitosan-based thin films is to exploit the ionic character of the polysaccharide to form polyelectrolyte multilayers (PEMs).[102,113–115] The simplest preparation approach consists in the alternate adsorption of oppositely charged species onto a charged substrate, known as layer-by-layer (LbL) deposition[116] (see Fig. 5A). The main driving force for the complexation of oppositely charged macromolecules is the entropic gain associated to the release of counterions,[117] a universal prerequisite for both synthetic and natural colloidal species.

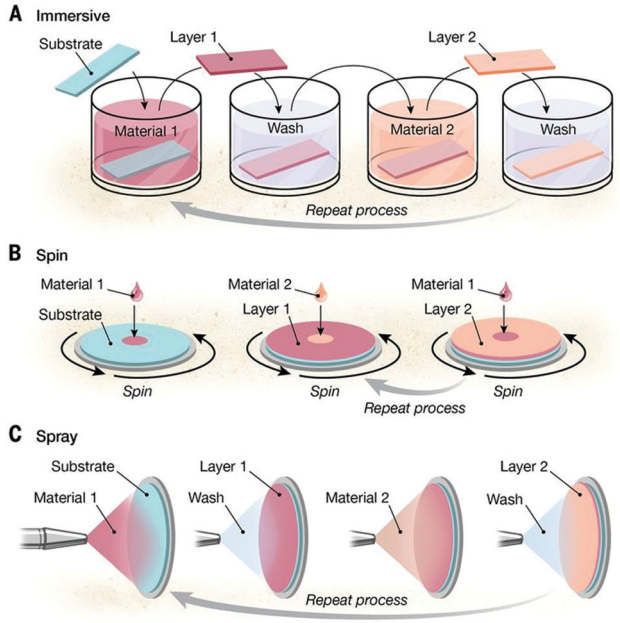

Fig. 5 Schematic illustration of different methods for the LbL assembly process: (A) dipping method, (B) consecutive spin-coating, and (C) spraying of oppositely charged polyelectrolytes. From ref. 113. Reprinted with permission from AAAS.

The ease of preparation and extreme versatility of the method come with a remarkably fine control of the film properties, such as thickness, roughness, internal layer structure, elasticity, and porosity, by selecting materials, solvent quality, pH, and ionic strength.[118,119]

Among the most popular combinations of chitosan with natural polyelectrolytes, we find alginate[120–123] and hyaluronic acid.[102,106,124] Alginate has the ability to form gels by ion bridges in the presence of multivalent cations, *e.g.*, calcium, due to the presence of carboxyl groups along the polymer backbone. Due to the porous structure and high water-absorption capacity of alginate-based assemblies, it is a promising and largely employed material for the design of wound dressings.[125] Concerning hyaluronic acid, it is almost ubiquitous in the human body and serves as an essential component mediating cellular signaling, wound repair, morphogenesis and matrix organization.[126] Furthermore, it is popular for its high flexibility, which becomes more relevant with increasing molecular weight.[127] Multilayers prepared from its combination with chitosan, which is known to participate in the up-regulation of genes related to calcium binding and mineralization promoting bone formation,[128] have been proposed to be used in potential "generic" surface treatment, since a simple variation of scaffold morphology, protein attachment and additive incorporation renders such films suitable for most tissue engineering applications.[112] Interestingly, the properties of the individual polyelectrolytes are partially retained in their surface properties, as evidenced by the surface hydrophilicity measured by water contact angle[106] (Fig. 6g), and it represents a convenient way to monitor the subsequent layer adsorption. A water contact angle between 80 and 100° is most commonly reported for chitosan-terminated PEMs, while the value decreases to 40–50° for alginate or hyaluronic acid termination.

Similar to synthetic weak polyelectrolytes,[129,130] the properties of both chitosan/alginate and chitosan/hyaluronic acid pairs are pH dependent, which allows the properties of the resulting films to be tuned. In particular, thicker and rougher layers can be formed at a pH between 3 and 5,[121] where the charge mismatch between low charge density chitosan and high charge density alginate (or hyaluronic acid) chains leads to the adsorption in a more coiled conformation. Such charge mismatch induces also larger mass adsorption to achieve charge neutralization.[131] The increment of surface roughness when chitosan/hyaluronan multilayers are used to coat solid substrates is very advantageous for cell adhesion, proliferation and differentiation, making them excellent bone scaffolds.[132] Regardless of the pH, the increase of ionic strength always results in the formation of thicker layers due to a stronger extrinsic charge compensation[123,133,134] and, analogous to synthetic polymers, ionic strengths below 10^{-4} mol L^{-1} prevent layer growth.[135]

The ensemble of characteristics of a deposition protocol, namely polymer molecular weight and architecture, ionic strength and type of ions, pH, and temperature, always defines the growth mechanism and the final properties of the multilayer, with the growth mechanism being an indication of the interaction strength within complexes. The low charge density, a consequence of the large intrinsic persistence length characteristic of chitosan, is the reason for the non-linear growth regime observed during the LbL deposition of several chitosan-based PEMs.[105,131] When the chitosan chains are loosely bound, they diffuse within the film, which enhances the mass uptake per adsorption cycle. The growth mechanism is therefore governed by the ability of chitosan to diffuse through the pre-adsorbed layers (in/out model),[136] with high MW chains diffusing less than their low MW equivalents.[131] A convenient way to highlight this two-step layer growth (adsorption and diffusion) is by monitoring the polyelectrolyte adsorption *in situ* by quartz crystal microbalance with dissipation monitoring (QCM-D) (Fig. 6e). The working principle of the technique exploits the piezoelectric properties of a quartz crystal under the application of an oscillating shear stress. The freely decaying damped sinusoidal oscillation of the crystal measured between subsequently applied shear deformations is registered and analysed with respect to the oscillation of an unloaded crystal. As a result of the mass coupled to the surface, the oscillation frequency f decreases, while the speed of the amplitude decay can be interpreted as a measure of the energy dissipated by the system coupled to the surface, *i.e.* the viscoelasticity of the film. The oscillation of the sensed mass has been a valid parameter to identify a typical behavior of highly diffusive polymers, which give very large mass uptake upon each adsorption step. This is the case of chitosan in combination with both alginate and hyaluronan, the layer growth of which can show a characteristic odd–even effect.[112,137] In addition to the diffusion through the film, such a behavior

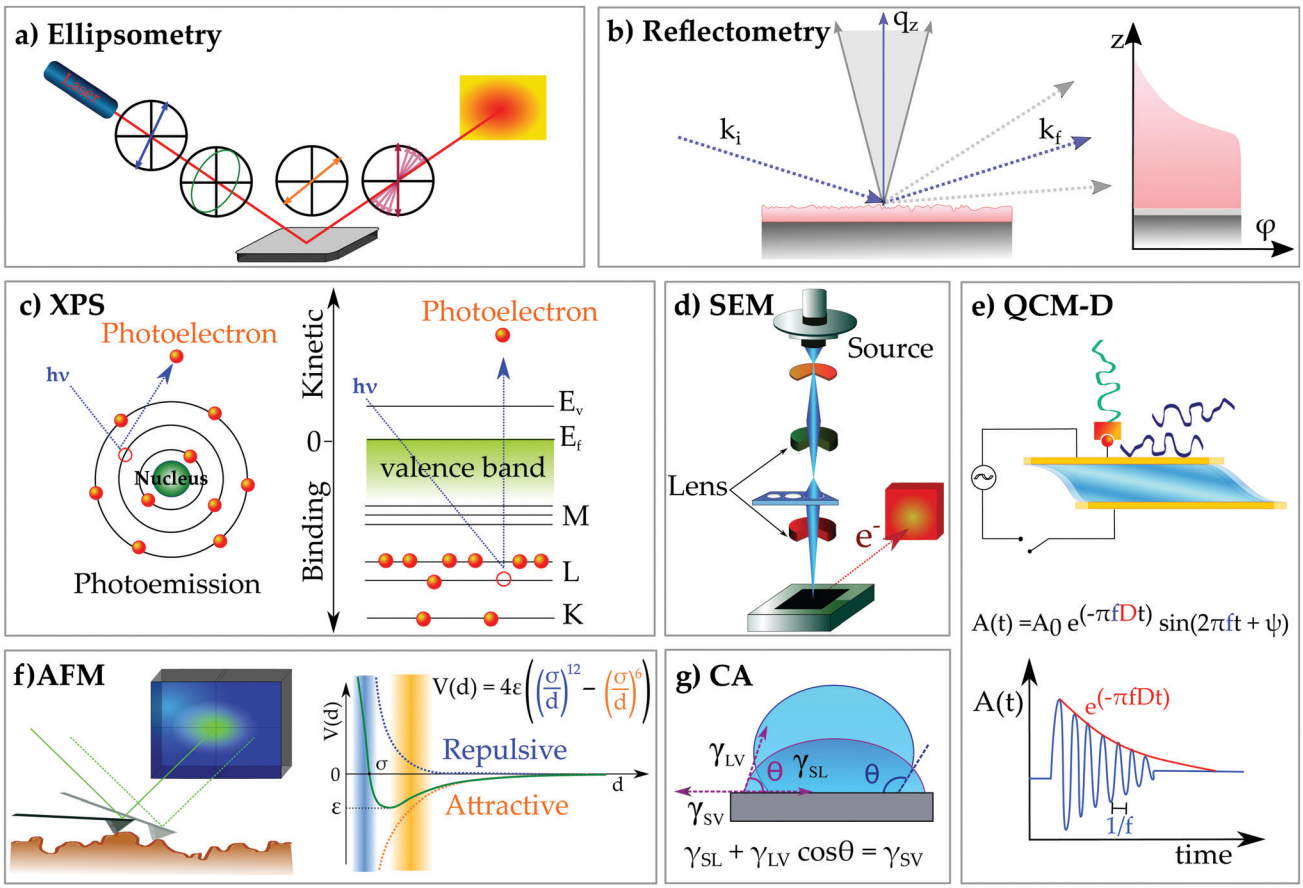

Fig. 6 Typical techniques for the characterization of thin films. (a) Ellipsometry is based on the detection of the change of polarization of light upon reflection from a substrate, which is described by the ellipsometric angles Δ and ψ. These parameters are related to the amplitude and the phase of the electromagnetic wave according to the fundamental equation: $\tan\psi \cdot \exp^{i\Delta} = r_p/r_s$ with r_p and r_s being the reflection coefficients of the perpendicular and parallel components of light, respectively. A layer model which describes the sample composition and its optical properties allow us to obtain the thickness d and refractive index n of the thin film from the experimental measurements. (b) Neutron or X-ray reflectometry provides information on the volume fraction distribution of molecules at interfaces. By measuring the reflected intensity of a probe (photons or neutrons) interacting with a solid surface at outgoing angles equal to the incoming one, a reflectivity profile in the reciprocal space, q_z, can be reconstructed. Characteristic structural parameters of a film like thickness (d), roughness σ and refractive index can be obtained by fitting the data to a proper model. The scattering properties of the components with respect to the incoming probe are described by the scattering length density ρ, which is correlated to the optical properties of the system by $\delta = \frac{\lambda^2}{2\pi}\rho$ with λ being the probe wavelength. (c) X-ray photoelectron spectroscopy provides information on the chemical composition of a specimen adsorbed onto a surface. It is based on the photoemission of electrons from an excited sample, the kinetic energy distribution of which is measured to derive the chemical composition and electronic state of the sample surface. By total energy transfer from the photons to the core-level electrons of atomic or molecular orbitals, these electrons are emitted from the sample surface and separated according to their energy, and so quantified. (d) Scanning electron microscopy uses a beam of electrons generated by an electron gun and guided through within vacuum in an electromagnetic field towards the specimen surface to study the morphological properties of a surface. When the beam strikes the specimen surface, its high energy electrons interact with the valence electrons of the atoms in the sample, and these are ejected (secondary electrons). These electrons are then translated in changes of the brightness of the corresponding point onto the screen, leading to the contrast of light and dark areas. (e) Quartz-crystal microbalance with dissipation monitoring (QCM-D) is a highly sensitive balance, which is able to detect nanograms of mass coupled to a substrate by detecting changes of the oscillation frequency of a quartz crystal. QCM-D uses the inverse piezoelectric effect, meaning that a driving sinusoidal potential is applied to a quartz crystal to excite the crystal oscillation forward and backward to its resonance frequency and higher overtones. When the potential is cut off, the damped amplitude of the freely decaying oscillation is recorded, and the frequency shift, Δf, and the dissipation energy, D, quantify the coupled mass and energy dissipated by the specimen. (f) Atomic force microscopy (AFM) measures the interaction between a specimen and a solid probe scanning over the surface in either static or dynamic (oscillating) mode. From its deflection of the probe, morphological features from the atomic to the macroscopic (millimeters) scale can be explored. The mapping of the surface topology is a reconstruction of the interaction forces, with near-field forces approximated to Lennard-Jones potentials. (g) Contact angle measurements are performed by depositing a droplet of a liquid, in most cases water, onto a bare or modified surface to determine its wetting behavior and therefore the surface hydrophilicity. The contact angle is defined as the geometrical angle between the substrate and the droplet, and it is correlated to the surface tension of all the involved interfaces by the Young equation.

can also be explained by the pronounced hydration of chitosan layers, responsible for the higher mass uptake (hydration water) and pronounced layer swelling,[114,121] therefore being well identifiable from the frequency shift/dissipation change upon layer formation and in combination with measurements of the "dry" mass by ellipsometry (Fig. 6a). Differently from chitosan, high charge density polymers like poly-L-lysine lead to a denser sequence of interaction sites per chain and stronger PE–PE

complexation at first contact[123] like the case of alginate/poly lysine complexes forming very compact PEMs.

Besides the association with biopolymers, fundamental studies of chitosan with synthetic polymers, for instance poly(acrylic acid), have been particularly useful.[138,139] One of these studies have highlighted another mechanism leading to the exponential growth: the formation of islands by the first deposited layers, which grow laterally and vertically with the number of deposition cycles.[119,136]

A fundamental aspect for (bio)technological applications of functional coatings is their stability under physiological and harsh conditions. For chitosan-based thin films, it has been observed that post-preparation stabilization *via* cross-linking is a valuable tool to enhance their mechanical and chemical stability under both acidic and alkaline conditions.[140,141] In addition to providing mechanical stability, cross-linking seems to control the extent of protein adsorption onto the modified substrate.[112,142] This possibility is not offered by all polymers, and it renders chitosan particularly interesting for post-synthetic modifications. Particularly relevant for regenerative tissue engineering and as antimicrobial surfaces[143] are those functional coatings combining chitosan with pectin. In this case, the 1 : 1 charge ratio achieved at pH 5.6 suppresses the chitosan diffusion and reduces its water uptake, which results in a linear thickness increment with initial mass uptake attachment and a slower chain rearrangement.[134] An important prerequisite for the film stability is that both polyelectrolytes are charged, and this corresponds to the pH between 3.6 and 7, and the salt concentration between 0.05 and 0.15 M NaCl.[144]

Another very promising system for regenerative medicine is represented by chitosan/collagen films. Collagen is a fibrous protein that plays an important role in tissue healing, providing a suitable biological environment for cell growth and attachment, migration, and proliferation.[145] Collagen thin films and low or high MW chitosans showed enhanced tensile strength and elongation at break compared to pure collagen films, as the intermolecular interactions within the matrix mitigate the strong intramolecular interaction within collagen chains, which increases the film flexibility.[146] Furthermore, chitosan contributes to preserve the native structure of collagen, limit hydrolytic and enzymatic degradation, and reduce the swelling of the collagen film (efficient moisture barrier), which could allow a controlled release of epidermal growth factors, when films are used as wound dressings.[146,147]

Among the rich variety of combinations of chitosan and other polysaccharides in thin films for biomedicine and biotechnology, it is worth mentioning the use of silk,[148] casein,[149] fucoidan,[111] cellulose,[150] and DNA.[151] In some cases, highly cross-linked structures, as confirmed by surface chemical characterization through X-ray photoelectron spectroscopy, are formed by reactive side groups. Furthermore, enhanced biofilm stability, like mucin, against degradation in surfactant solutions has been proven in the presence of chitosan, as the interactions with the polysaccharide reduce the hydrophobic interactions with the surfactant molecules and preserve the binding to the solid substrates.[152] Finally, the possibility of driving the assembly of inorganic nanoparticles (NPs), *e.g.* gold (Au)-NPs,[153] for the preparation of surface electrodes and impedance spectroscopy studies has also been reported, which is added to the numerous examples of highly relevant applications of chitosan-based thin films for the design of bioengineering surfaces, among which are antimicrobial surface[102,103,154] and modulated drug release,[102] biosensing,[155] anticancer treatment,[156] anticoagulant for implants in cardiovascular surgery,[157] food preservation,[110,158] lubrication,[99] release of fertilizers,[159] and flame retardants.[107]

For most of these applications, simple preparation methods, simple to speed and scale up for industrial purposes, are fundamental, and therefore alternate or simultaneous spin-coating or spraying of polyelectrolyte solutions[160] is a valid alternative to the LbL deposition (Fig. 5B and C). Spraying polyelectrolyte solutions onto a substrate leads to similar structures as dipped multilayers, with minor differences in the growth kinetics of the very first layers due to the suppression of diffusive events,[161,162] which results in thinner and smoother layers, as revealed by atomic force and fluorescence microscopy of synthetic polyelectrolytes,[163,164] and it has been successfully applied to prepare chitosan-based multilayers onto flat[100,165] or curved surfaces.[159] The shape and dimensions of chitosan:polyanion complexes remain crucial parameters for the film buildup by either alternate or simultaneous spraying, and they can be properly tuned by the mixing ratio and physico-chemical bulk properties.

The peculiarity of charge inversion from the cationic to the anionic form by proper chemical derivation has awarded the possibility of self-assembling ''one component'' multilayers, fully based on chitosan.[166] The resulting thin films were very smooth and characterized by a linear layer increment, due to the equal charge density along the chain between polyanionic and polycationic forms. Interestingly, their complexation was more exothermic (lower ΔH_{mix}) and more entropically favored (higher ΔS_{mix}) than that for other chitosan/synthetic PE pair, resulting in an overall enhanced film stability.

Less popular than the LbL deposition, another method for thin film preparation is the Langmuir–Blodgett technique. In this case, a Langmuir monolayer is formed by spreading an amphiphilic (macro)molecule dissolved in a volatile organic solvent on the surface of an aqueous subphase.[167] The molecules orient their hydrophilic part in the aqueous subphase and the hydrophobic moiety towards the hydrophobic phase (air). Such a monolayer is then transferred onto a solid substrate by the Langmuir–Blodgett (LB) process[168] by immersing (or emerging) a solid support in (or from) the aqueous subphase to recover the monolayer, with the possible formation of multilayers by multiple dipping iterations. LB multilayers have been prepared from amphiphilic chitosan derivatives, as well as their mixtures with phospholipids and cholesterol.[169] In this case, chemical modifications are a fundamental prerequisite to render chitosan soluble in organic solvents, and most frequently long alkyl chains are attached to the primary hydroxyl and amino group for this purpose.[169,170]

The highly tunable structure of chitosan:fatty acid complexes in solution, forming multiwalled vesicles, was prepared in bulk under tailored conditions (pH and mixing ratio) to obtain the desired dimensions and number of layers,[31] which have been the key properties for the development of a novel approach for the preparation of chitosan–surfactant multilayers from "one step" deposition, as schematically represented in Fig. 7.[33] This method overcomes the limitation of time consuming LbL assembly and offers more control over the internal layer structure than spraying methods. Chitosan:fatty acid complexes were then transferred onto a solid substrate by a single spin coating step, which spontaneously formed multilayers with a high degree of interlayer segregation. The control of structural key parameters, *e.g.* thickness and number of layers, from the bulk properties of the mixture ease significantly the preparation of films with tailored properties and functions. Furthermore, the low degree of intermixing between subsequent layers leading to high layer segregation makes this kind of multilayer suitable for selective release/uptake and exclusive response of individual parts to external stimuli. The highly segregated internal structure with individual water uptake of the hydrophilic moieties (chitosan layers) could be revealed only by exploiting the isotopic contrast of neutron reflectometry. In general, both X-ray and neutron reflectometry allow the determination of the internal volume fraction distribution of each component along the axis perpendicular to the surface. Their complementarity is due to the fact that their probes, photons and neutrons, interact with different subatomic elements of an atom (the electron cloud and the nuclei, respectively) and therefore provide a different internal contrast of the same systems. In addition, neutrons interact differently with isotopes of the same nucleus, and this property can be used as a tool for identifying the internal structures of chemically homogeneous materials.

Our results showed that the morphology of coatings produced by this method is macroscopically highly homogeneous, but it phase separates microscopically on a length scale of 5 nm. The electrostatic interaction between the amino-group of chitosan and the carboxylic termination of the fatty acids and the very low miscibility of chitosan with both hydrophilic and hydrophobic materials are at the origin of the very small-scale segregation. Since the size of the microseparated domains depends on the degree of polymerization of the polymer and on the Flory–Huggins interaction parameter(s) χ with different film components, a common strategy to prepare thin films with sub-10 nm structural features, essential for novel applications in nanolithography, is to use oligosaccharide based block copolymers.[171,172]

Finally, the preparation of chitosan thin films from end-tethering polymer chains onto a solid surface, a geometry known as polymer brush,[173,174] is worth mentioning. Either neutral or modified chitosan chains by quaternary ammonium salts, CHI-Q$_x$, were grafted to the epoxide derivatized silicon oxide surface,[175,176] with characteristic dry thickness from 5 to 50 nm from fully charged (CHI-Q$_{100}$) to partial (CHI-Q$_{50}$, CHI-Q$_{25}$) to neutral brushes, respectively, due to a decreased grafting density for a higher charge density. An interesting property of polymer brushes is their swelling behavior, which can be exploited to design (bio)sensors and microactuators. These chitosan-based brushes have shown a variable swelling behavior over a broad pH range as a function of their quaternization form, with CHI-Q$_{100}$ swelling up to 5 times their dry thickness at pH 5 and with an intermediate swelling degree symmetrically around this pH. Partially modified CHI-Q$_{50}$ brushes were swelling symmetrically around pH 4.5, which is likely due to the balance between increasing protonation of primary amines below pH 6.5 and quaternary ammonium salts

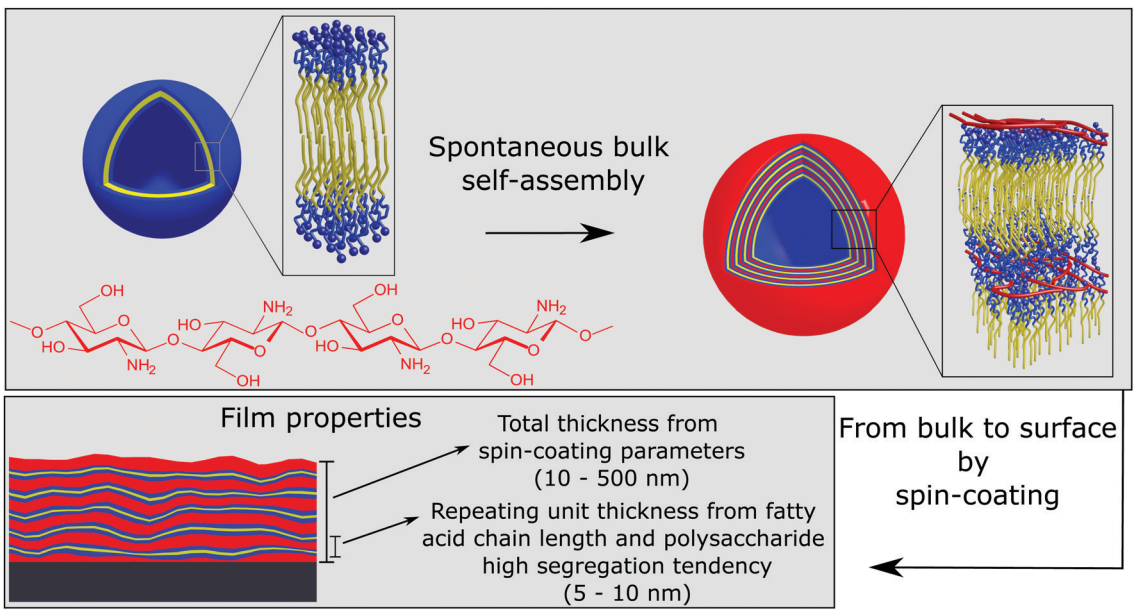

Fig. 7 Schematic representation of the formation of chitosan/fatty acid multilayered thin films *via* a one-step procedure which exploits the spontaneous association of the components into multilayered vesicles in solution. Adapted with permission from ref. 33.

above pH 6.5. In contrast, the swelling of native chitosan and CH-Q_{25} was constant from pH 8.2 to 5.5 and increases near pH 4. The swelling behavior could be rationalised in terms of the size of the counterions condensed around the charged groups: for fully protonated brushes, the swelling clearly increases with the size of counterions, while for partially protonated brushes the influence of the ions is evident at high pH, where there is a complete exchange of counterions from chloride to hydroxide, which have larger hydration shells. Such an effect is not visible for conditions of low pH and a low degree of quaternization, where the ammonium cation content is below a critical value.

Chitosan brushes also exhibited a reduced bacterial attachment/growth of about 30 times compared to the silane (APTES)-modified surface, which has been explained by the capability of the quaternary salt of disrupting the bacterial cell membrane, as well as by the flexible nature of polymer brushes.[177] In fact, *S. aureus* biofilms adhered strongly to silicon oxide and CH surfaces even at a high shear stress (up to 12 dyne per cm^2), whereas they detached at a low shear stress (1.5 dyne per cm^2).

Brushes were prepared also from chitosan-grafted-poly(ethylene glycol) (PEG) copolymers,[178,179] reaching a very high degree of substitution, and adsorbed onto a thiol-modified gold substrate by microcontact printing, covalent grafting and solution adsorption, with the latter leading to the highest polymer adsorption. The presence of PEG units has been crucial to reach high surface adsorption, as revealed by QCM-D studies, and it enhances the hydration degree of chitosan thin films.

Chitosan-based nanocomposites and solid films

The combination of polymers and inorganic nanoparticles represents a well-known strategy to obtain hybrid materials with unique performances as well as specific functionalities. Among sustainable polymers, chitosan was largely employed as a matrix for the fabrication of bionanocomposites suitable for several applications, such as tissue engineering,[180,181] drug delivery,[182,183] gas sensors,[184] packaging,[185,186] remediation[187,188] and cultural heritage.[189,190] Such a wide industrial interest is related to some interesting features of chitosan itself in the solid state. In particular, chitosan and its phosphorylated derivative are flame retardant and therefore they are perspective additives to control the flammability properties of polyethylene or to produce self-extinguishing cotton fabrics.[191–193] Additionally, chitosan, being a polycation, has a broad-spectrum antimicrobial activity against both Gram-positive and Gram-negative bacteria as well as fungi that can be further enhanced by transforming the primary amine groups into quaternary salts with permanent positive charge.[194]

The mechanical performance of chitosan composites is affected by the crystallinity that has a great influence on tensile strength. Therefore, chitosan films fabricated through solvent casting from acetic acid may have significant differences in mechanical properties if DDA, pH and water content in the final composite (relative humidity), which highly influence the polymer crystallinity, are altered.[195,196]

Besides the chemical modification of the chitosan structure, both natural and synthetic nanoparticles were successfully filled within the chitosan matrix to tune its properties. The nanocomposite preparation includes physical and chemical methods.[198] Metal nanoparticles (Cu, Ag and Au) were embedded in chitosan through the following subsequent steps:[199] (1) metal vapour synthesis for the preparation of the metal nanoparticle sols and (2) deposition of the metal nanoparticle sols on chitosan supports. Chitosan/ZnO nanocomposites were fabricated by the microwave heating technique,[187] which reduced the reaction time for the ligand substitution occurring between the functional groups of the biopolymer and the zinc cations of ZnO nanoparticles. The addition of ZnO nanoparticles improved the removal capacity of chitosan towards methylene blue.[187] The freeze-drying process was employed for the filling of nano-hydroxyapatite particles within the chitosan matrix,[200] while the ultrasonic-assisted method was used for the fabrication of composite scaffolds based on the chitosan hydrogel and multiwalled carbon nanotubes (MWCNTs).[181] The addition of nano-hydroxyapatite improved the compression behaviour of the chitosan scaffold in terms of elasticity and flexibility.[200] A multifunctional hybrid material composed by chitosan, graphene oxide (GO) and iron oxide (IO) was obtained by the hydrothermal method exploiting the 1-ethyl-3-(3-dimethylaminopropyl) carbodiimide (EDC) reaction chemistry.[201] The chitosan–GO–IO nanocomposite revealed an efficient antimicrobial ability towards both Gram-positive (*Staphylococcus aureus*) and Gram-negative (*Escherichia coli*) bacteria.[201] Due to its super-paramagnetic properties, the chitosan–GO–IO hybrid can be easily separated from the bacteria and reutilized for subsequent biocide applications.[201]

The aqueous casting method was largely employed in the fabrication of chitosan based nanocomposites containing natural clay nanoparticles, such as kaolinite nanosheets[202,203] and halloysite nanotubes (HNTs).[203–205] A previous study[180] reports that the amino-modification of the halloysite outer surface can favour the chitosan/HNT interfacial interactions allowing hybrid films with excellent tensile and thermal properties to be obtained. Additionally, the amino-modified clay nanotubes strongly improved the water vapour transmission rate of chitosan, making the bionanocomposite films promising for biomedical purposes.[180] Ethylene glycol diglycidyl ether (EGDE) was used as a cross-linker for the preparation of chitosan/amino-modified halloysite composite films. In the process, the hollow tubular shape of halloysite HNTs-NH_2 was not altered by the amino functionalization, and the composite film exhibits a porous structure, as shown by scanning electron microscopy (Fig. 8a). It was observed that the swelling ratio of chitosan based nanocomposites decreases with the HNTs-NH_2 content (Fig. 8b).

Within tissue engineering applications, a chitosan/halloysite composite scaffold was fabricated by the combination of solution-mixing and freeze-drying techniques.[206] The presence of clay nanotubes induced an improvement of both the compressive

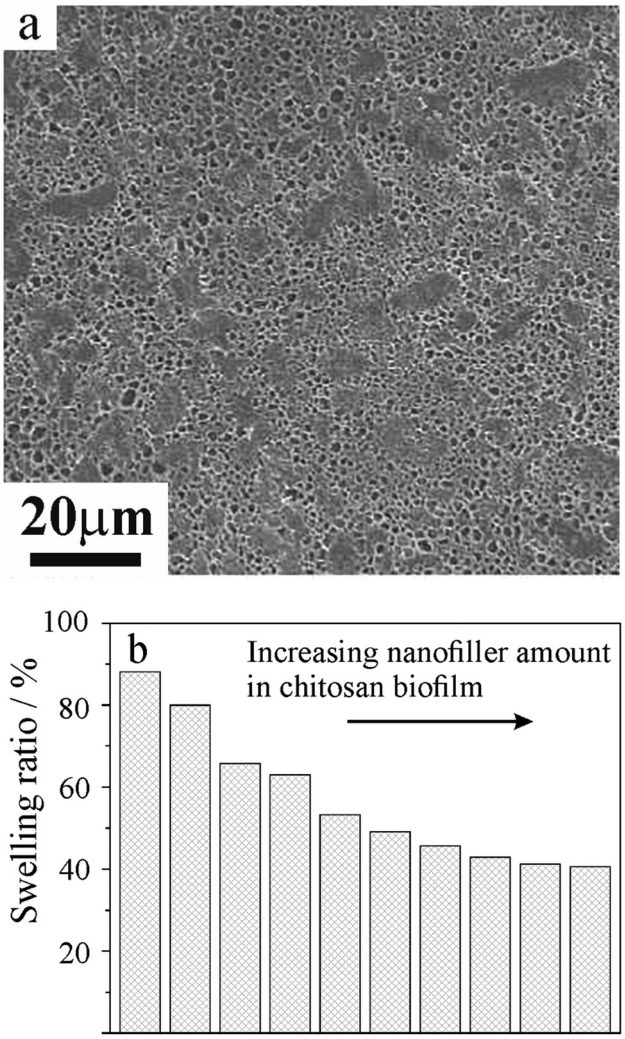

Fig. 8 (a) SEM image of the chitosan/HNTs-NH_2 nanocomposite film containing ethylene glycol diglycidyl ether (EGDE) as the cross-linking agent. (b) The swelling ratio of chitosan/HNTs-NH_2 nanocomposite films. Adapted from ref. 180, coryright 2020, with permission from Elsevier

behaviour (in terms of strength and Young modulus) and the thermal stability with respect to the scaffold based on pristine chitosan.[206] Nanoclays with variable morphology (bentonite, sepiolite, and montmorillonite) were successfully filled into chitosan blended with glycerol by using the casting technique from water.[207] Similarly, the chitosan/polyvinyl alcohol (PVA) blend was reinforced with different concentrations of bentonite nanoparticles combined with anthocyanin in order to obtain antibacterial films with improved thermo-mechanical performances.[183] The casting procedure was effective in the preparation of films composed by copper oxide (CuO) nanoparticles and chitosan doped with glycerol ionic liquid.[184]

Recently, chitosan/halloysite nanocomposite films with a sandwich-like structure, as sketched in Fig. 9a, were fabricated by using a sequential casting method.[197] The preparation protocol is based on the sequential deposition of chitosan and halloysite aqueous suspensions under controlled pH conditions. SEM images (Fig. 9b) showed that the nanocomposite possesses a multilayer morphology being that halloysite nanotubes are confined between the outer chitosan layers. Compared to pure chitosan, a significant increase (up to *ca.* 150 °C) of the ignition temperature, as well as the enthalpy of the oxidation (Fig. 9c), was detected in the hybrid films as a consequence of their layered structure.[197] The flame retardant features of materials where the polymer and inorganic particles, typically clays, are alternated are well known but a large number of multilayers with micro/nanosized thickness is required;[208] on the other hand, the flame retardant features of the chitosan itself combined with the peculiar pH dependent solubility endow the reduction of flammability in more simple layered structures that are easy to generate. Accordingly, the sequential casting procedure can be considered a successful protocol to fabricate chitosan based nanocomposites with flame retardant properties.

Nanocomposite films formed using the chitosan/polyvinyl alcohol (PVA) blend as the matrix and graphene oxide/hydroxyapatite/gold nanoparticles as fillers were prepared by the gel casting method using glutaraldehyde as the crosslinker.[209] These bionanocomposite films are promising for bone tissue regeneration as evidenced by the MTT assays and ALP straining results, which evidenced their capacity to enhance the osteoblast differentiation.[209] Within biomedical applications, the addition of rectorite clay particles into chitosan allowed a composite viscous mucus with injectable properties for skin hemostasis to be obtained,[210] whereas montmorillonite clay was introduced to the methacrylated glycol chitosan (MeGC) hydrogel, which was obtained by using riboflavin as a photoinitiator.[211] The composite hydrogel evidenced a well interconnected microporous structure promoting the cell infiltration, proliferation, and *in situ* differentiation.[211] Hybrid gel beads based on chitosan and halloysite were prepared through the dropping and pH-precipitation method, which is based on the drop-wise addition of chitosan/halloysite dispersion into an aqueous NaOH solution.[182,188] The chitosan/HNT gel beads exhibited higher adsorption capacities towards dyes (methylene blue and malachite green) with respect to those of chitosan gel beads.[188] As concerns pharmaceutical purposes, chitosan/HNT gel beads were shown to be efficient in the controlled release of doxycycline (an antibiotic of the tetracycline class), highlighting their suitability as a drug delivery system.[188] Interestingly, drug release can be extended by covering the surface of the chitosan/HNT gel beads with alginate exploiting the electrostatic attractions occurring between the biopolymers, which are oppositely charged.[188] Regarding Cultural Heritage, hybrid gels with surface cleaning ability were fabricated by mixing a chitosan aqueous solution with a Pickering emulsion based on HNTs and *n*-decane.[189] It should be noted that a subsequent drop-wise addition of NaOH solution was conducted to obtain the gel phase from the chitosan/HNTs/*n*-decane mixture.[189]

Summary and perspectives

Chitosan exhibits a unique set of physico-chemical characteristics, most notably its low solubility, high intrinsic rigidity,

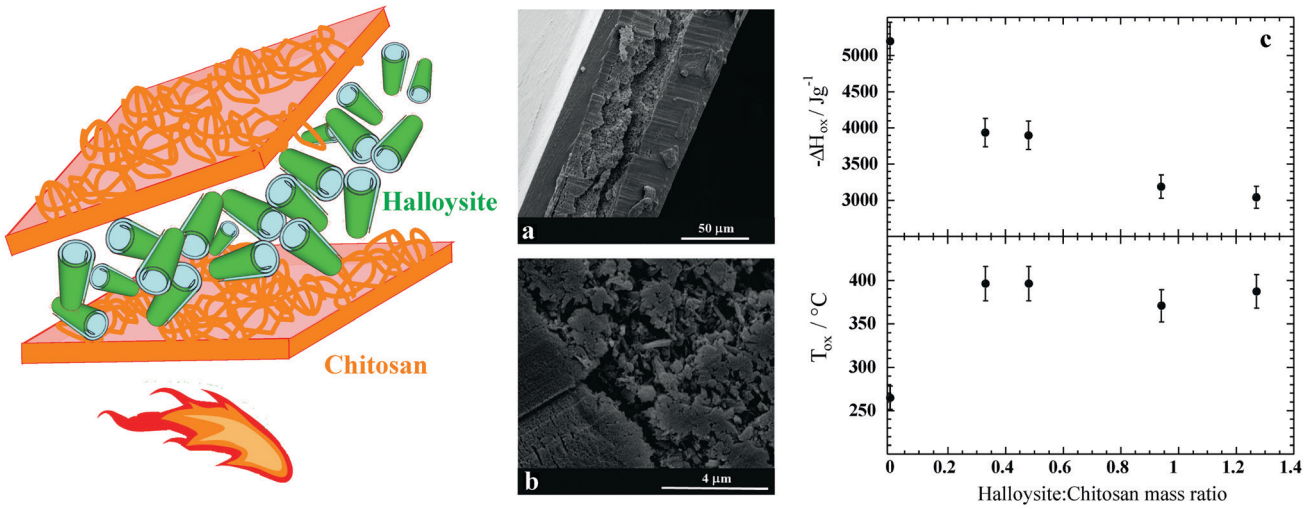

Fig. 9 Schematic representation of the chitosan/HNT nanocomposites with a layered structure. (a and b) SEM micrographs at different magnifications of the cross section of chitosan/HNT nanocomposites with a mass ratio of 0.62. (c) Enthalpy and onset temperature of oxidative degradation as functions of the HNT/chitosan mass ratio for the layered nanocomposites. Adapted with permission from ref. 197.

large charge separation, and strong tendency to form intra- and intermolecular hydrogen bonds. In this contribution, an overview of recent advances in chitosan-based materials is presented, whereby attention has been paid to clarifying how the peculiarities of chitosan affect the physico-chemical properties of the resulting materials.

The focus of the review was placed on chitosan-based aqueous systems, thin films, and composite materials. Few polymers have attracted comparable attention and have been used for the design of so different systems. Accordingly, an overwhelming amount of literature appears each year on the topic. Similarly, the number of patents involving chitosan is continuously growing, indicating that chitosan not only attracts the interest of the scientific community but also finds wide practical application. Chitosan is abundant (second to cellulose among biopolymers), competitive for physico-chemical properties and its use fits the idea of a circular economy as it is a byproduct of the food industry.

A contrast, commonly found in the field of materials science, is that the rapid development of applications goes with a comparably slow progress in the understanding of the fundamental properties of the investigated system. Chitosan makes no exception to this rule. In fact, very fundamental questions about chitosan remain unanswered. For instance, a random distribution of *N*-acetylamine units along the polymer backbone is assumed, despite the fact that no evidence for chitosan being a random copolymer was ever presented. From a biological viewpoint, the mechanisms of interaction of chitosan with cell, bacteria, and plants are not well understood and therefore a discrepancy in the reproducibility of bioactivity is observed. It seems clear that although several mechanisms of action are reported, the most established idea is that electrostatic interactions between chitosan and the anionic molecules of cells/DNA may control the bioactivity instead of interactions with a specific receptor.

Moreover, the interactions determining the behavior of hybrid systems can strongly vary: from non-specific, long range, electrostatic interactions, through more specific hydrogen bonds, to short-range and highly directional ionic bridges. Such a diversity makes systematic studies difficult to perform and predictions hardly apply to a broad variety of systems. Clearly, a better understanding of the behavior of this macromolecule is needed to improve our capacity to design chitosan-based materials. In conclusion, it is generally true that the physical and chemical properties of chitosan-based materials can be rationalized on the basis of the physico-chemical properties of this important bio-macromolecule. It is equally true that further fundamental and applied studies are required to improve our capacity to predict the properties of highly complex, multi-component, chitosan based materials.

Conflicts of interest

There are no conflicts to declare.

Acknowledgements

The work was financially supported by Progetto di ricerca e sviluppo "AGM for CuHe" (ARS01_00697) and University of Palermo. The experimental work performed on chitosan–fatty acid complexes and thin films has profited from the laboratory infrastructure provided by the Partnership of Soft Condensed Matter (PSCM) at the Institut Laue-Langevin.

References

1 M. Rinaudo, *Prog. Polym. Sci.*, 2006, **31**, 603–632.
2 C. Tang, N. Chen, Q. Zhang, K. Wang, Q. Fu and X. Zhang, *Polym. Degrad. Stab.*, 2009, **94**, 124–131.

3 K. B. Mukhtar Ahmed, M. M. A. Khan, H. Siddiqui and A. Jahan, *Carbohydr. Polym.*, 2020, **227**, 115331.
4 M. Rinaudo, M. Milas and P. Le Dung, *Int. J. Biol. Macromol.*, 1993, **15**, 281–285.
5 C. Schatz, C. Viton, T. Delair, C. Pichot and A. Domard, *Biomacromolecules*, 2003, **4**, 641–648.
6 H. Wang, J. Qian and F. Ding, *J. Mater. Chem. B*, 2017, **5**, 6986–7007.
7 Y. P. Singh, J. C. Moses, N. Bhardwaj and B. B. Mandal, *J. Mater. Chem. B*, 2018, **6**, 5499–5529.
8 F. Khan, D. T. N. Pham, S. F. Oloketuyi, P. Manivasagan, J. Oh and Y.-M. Kim, *Colloids Surf., B*, 2020, **185**, 110627.
9 W. Zhang, H. Wang, X. Hu, H. Feng, W. Xiong, W. Guo, J. Zhou, A. Mosa and Y. Peng, *J. Cleaner Prod.*, 2019, **231**, 733–745.
10 L. Xing, Y.-T. Fan, L.-J. Shen, C.-X. Yang, X.-Y. Liu, Y.-N. Ma, L.-Y. Qi, K.-H. Cho, C.-S. Cho and H.-L. Jiang, *Int. J. Biol. Macromol.*, 2019, **141**, 85–97.
11 M. Nasrollahzadeh, N. Shafiei, Z. Nezafat, N. S. Soheili Bidgoli and F. Soleimani, *Carbohydr. Polym.*, 2020, **241**, 116353.
12 L. Xu, C. Wang, Y. Cui, A. Li, Y. Qiao and D. Qiu, *Sci. Adv.*, 2019, **5**, eaau3442.
13 M. Rinaudo, N. R. Kil'deeva and V. G. Babak, *Russ. J. Gen. Chem.*, 2008, **78**, 2239–2246.
14 L. Chiappisi, I. Hoffmann and M. Gradzielski, *Soft Matter*, 2013, **9**, 3896–3909.
15 L. Chiappisi and M. Gradzielski, *Adv. Colloid Interface Sci.*, 2015, **220**, 92–107.
16 C. Onesippe and S. Lagerge, *Carbohydr. Polym.*, 2008, **74**, 648–658.
17 Y. C. Wei and S. M. Hudson, *Macromolecules*, 1993, **26**, 4151–4154.
18 L. Petrović, J. Milinković, J. Fraj, S. Bučko, J. Katona and L. Spasojević, *Colloid Polym. Sci.*, 2017, **295**, 2279–2285.
19 S. Peretz, M. Florea-Spiroiu, D.-F. Anghel, C. Munteanu, D. Angelescu, C. Stoian and G. Zgherea, *J. Appl. Polym. Sci.*, 2014, **131**, 40059.
20 P. Pal and A. Pal, *Int. J. Biol. Macromol.*, 2017, **104**, 1548–1555.
21 S. Demarger-André and A. Domard, *Carbohydr. Polym.*, 1994, **23**, 211–219.
22 M. C. Bonferoni, G. Sandri, E. Dellera, S. Rossi, F. Ferrari, M. Mori and C. Caramella, *Eur. J. Pharm. Biopharm.*, 2014, **87**, 101–106.
23 M. Vargas, A. Albors, A. Chiralt and C. González-Martínez, *Food Hydrocolloids*, 2009, **23**, 536–547.
24 E. Dellera, M. C. Bonferoni, G. Sandri, S. Rossi, F. Ferrari, C. Del Fante, C. Perotti, P. Grisoli and C. Caramella, *Eur. J. Pharm. Biopharm.*, 2014, **88**, 643–650.
25 M. V. Shamov, S. Y. Y. Bratskaya and V. A. Avramenko, *J. Colloid Interface Sci.*, 2002, **249**, 316–321.
26 S. Demarger-André and A. Domard, *Carbohydr. Polym.*, 1995, **27**, 101–107.
27 I. Ahmed, L. Dildar, A. Haque, P. Patra, M. Mukhopadhyay, S. Hazra, M. Kulkarni, S. Thomas, J. R. Plaisier, S. B. Dutta and J. K. Bal, *J. Colloid Interface Sci.*, 2018, **514**, 433–442.
28 M. Hasan, G. Ben Messaoud, F. Michaux, A. Tamayol, C. J. F. Kahn, N. Belhaj, M. Linder and E. Arab-Tehrany, *RSC Adv.*, 2016, **6**, 45290–45304.
29 H. W. Tan and M. Misran, *J. Liposome Res.*, 2012, **22**, 329–335.
30 L. Chiappisi, S. Prévost, I. Grillo and M. Gradzielski, *Langmuir*, 2014, **30**, 1778–1787.
31 L. Chiappisi, S. Prévost, I. Grillo and M. Gradzielski, *Langmuir*, 2014, **30**, 10608–10616.
32 L. Chiappisi, S. David Leach, M. Gradzielski, S. D. Leach and M. Gradzielski, *Soft Matter*, 2017, **13**, 4988–4996.
33 S. Micciulla, D. W. Hayward, Y. Gerelli, A. Panzarella, R. von Klitzing, M. Gradzielski and L. Chiappisi, *Commun. Chem.*, 2019, **2**, 61.
34 L. Chiappisi, M. Simon and M. Gradzielski, *ACS Appl. Mater. Interfaces*, 2015, **7**, 6139–6145.
35 M. Valtiner, S. H. Donaldson, M. A. Gebbie and J. N. Israelachvili, *J. Am. Chem. Soc.*, 2012, **134**, 1746–1753.
36 J. H. J. Hamman, *Mar. Drugs*, 2010, **8**, 1305–1322.
37 Y. Luo and Q. Wang, *Int. J. Biol. Macromol.*, 2014, **64**, 353–367.
38 P. Pakornpadungsit, T. Prasopdee, N. M. Swainson, A. Chworos and W. Smitthipong, *Polym. Test.*, 2020, **83**, 106333.
39 L. M. Bravo-Anaya, K. G. Fernández-Solís, J. Rosselgong, J. L. E. Nano-Rodríguez, F. Carvajal and M. Rinaudo, *Int. J. Biol. Macromol.*, 2019, **126**, 1037–1049.
40 P. L. Ma, M. Lavertu, F. M. Winnik and M. D. Buschmann, *Carbohydr. Polym.*, 2017, **176**, 167–176.
41 J.-W. Shen, J. Li, Z. Zhao, L. Zhang, G. Peng and L. Liang, *Sci. Rep.*, 2017, **7**, 5050.
42 P. L. Ma, M. Lavertu, F. M. Winnik, M. D. Buschmann, L. M. Pei, M. Lavertu, F. M. Winnik and M. D. Buschmann, *Biomacromolecules*, 2009, **10**, 1490–1499.
43 H. Ragelle, R. Riva, G. Vandermeulen, B. Naeye, V. Pourcelle, C. S. Le Duff, C. D'Haese, B. Nysten, K. Braeckmans, S. De Smedt, C. Jérôme and V. Préat, *J. Controlled Release*, 2014, **176**, 54–63.
44 I. Pilipenko, V. Korzhikov-Vlakh, V. Sharoyko, N. Zhang, M. Schäfer-Korting, E. Rühl, C. Zoschke and T. Tennikova, *Pharmaceutics*, 2019, **11**, 317.
45 C. Zandanel, M. Noiray and C. Vauthier, *Pharm. Res.*, 2020, **37**, 22.
46 P. Holzerny, B. Ajdini, W. Heusermann, K. Bruno, M. Schuleit, L. Meinel and M. Keller, *J. Controlled Release*, 2012, **157**, 297–304.
47 S. Reed and B. M. Wu, *J. Biomed. Mater. Res., Part B*, 2017, **105**, 272–282.
48 K. Xu, K. Ganapathy, T. Andl, Z. Wang, J. A. Copland, R. Chakrabarti and S. J. Florczyk, *Biomaterials*, 2019, **217**, 119311.
49 E. A. Krisanti, G. M. Naziha, N. S. Amany, K. Mulia and N. A. Handayani, *IOP Conf. Ser.: Mater. Sci. Eng.*, 2019, **509**, 012100.
50 M. Kuczajowska-Zadrożna, U. Filipkowska and T. Jóźwiak, *J. Environ. Chem. Eng.*, 2020, 103878.

51 A. B. Kayitmazer, A. F. Koksal and E. Kilic Iyilik, *Soft Matter*, 2015, **11**, 8605–8612.
52 O. Karabiyik Acar, A. B. Kayitmazer and G. Torun Kose, *Biomacromolecules*, 2018, **19**, 1198–1211.
53 C. Schatz, J.-M. Lucas, C. Viton, A. Domard, C. Pichot and T. Delair, *Langmuir*, 2004, **20**, 7766–7778.
54 J. Valente, V. Gaspar, B. Antunes, P. Countinho and I. Correia, *Polymer*, 2013, **54**, 5–15.
55 P. M. de la Torre, S. Torrado and S. Torrado, *Biomaterials*, 2003, **24**, 1459–1468.
56 Q. Chen, Y. Hu, Y. Chen, X. Jiang and Y. Yang, *Macromol. Biosci.*, 2005, **5**, 993–1000.
57 Y. Hu, X. Jiang, Y. Ding, H. Ge, Y. Yuan and C. Yang, *Biomaterials*, 2002, **23**, 3193–3201.
58 R.-Y. Zhang, E. Zaslavski, G. Vasilyev, M. Boas and E. Zussman, *Biomacromolecules*, 2018, **19**, 588–595.
59 D. Chuan, T. Jin, R. Fan, L. Zhou and G. Guo, *Adv. Colloid Interface Sci.*, 2019, **268**, 25–38.
60 S. P. Strand, S. Lelu, N. K. Reitan, C. de Lange Davies, P. Artursson and K. M. Vårum, *Biomaterials*, 2010, **31**, 975–987.
61 C. Cui, C. Shao, L. Meng and J. Yang, *ACS Appl. Mater. Interfaces*, 2019, **11**, 39228–39237.
62 S. Gokila, T. Gomathi, P. Sudha and S. Anil, *Int. J. Biol. Macromol.*, 2017, **104**, 1459–1468.
63 D. P. Facchi, A. L. Cazetta, E. A. Canesin, V. C. Almeida, E. G. Bonafé, M. J. Kipper and A. F. Martins, *Chem. Eng. J.*, 2018, **337**, 595–608.
64 F.-L. Mi, H.-W. Sung and S.-S. Shyu, *Carbohydr. Polym.*, 2002, **48**, 61–72.
65 K. Baysal, A. Z. Aroguz, Z. Adiguzel and B. M. Baysal, *Int. J. Biol. Macromol.*, 2013, **59**, 342–348.
66 W. Zhang, X. Jin, H. Li, R.-R. Zhang and C.-W. Wu, *Carbohydr. Polym.*, 2018, **186**, 82–90.
67 R. Rodríguez-Rodríguez, H. Espinosa-Andrews, C. Velasquillo-Martínez and Z. Y. García-Carvajal, *Int. J. Polym. Mater. Polym. Biomater.*, 2020, **69**, 1–20.
68 H. Hamedi, S. Moradi, S. M. Hudson and A. E. Tonelli, *Carbohydr. Polym.*, 2018, **199**, 445–460.
69 P. Mohammadzadeh Pakdel and S. J. Peighambardoust, *Carbohydr. Polym.*, 2018, **201**, 264–279.
70 N. Sereni, A. Enache, G. Sudre, A. Montembault, C. Rochas, P. Durand, M. H. Perrard, G. Bozga, J. P. Puaux, T. Delair and L. David, *Langmuir*, 2017, **33**, 12697–12707.
71 A. A. Enache, L. David, J. P. Puaux, I. Banu and G. Bozga, *J. Appl. Polym. Sci.*, 2018, **135**, 1–12.
72 P. Sacco, F. Brun, I. Donati, D. Porrelli, S. Paoletti and G. Turco, *ACS Appl. Mater. Interfaces*, 2018, **10**, 10761–10770.
73 Y. Huang, Y. Cai and Y. Lapitsky, *J. Mater. Chem. B*, 2015, **3**, 5957–5970.
74 P. Sacco, S. Paoletti, M. Cok, F. Asaro, M. Abrami, M. Grassi and I. Donati, *Int. J. Biol. Macromol.*, 2016, **92**, 476–483.
75 L. Bugnicourt and C. Ladavière, *Prog. Polym. Sci.*, 2016, **60**, 1–17.
76 L. Dambies, T. Vincent, A. Domard and E. Guibal, *Biomacromolecules*, 2001, **2**, 1198–1205.
77 Azizullah, N. ur Rehman, A. Haider, U. Kortz, S. U. Afridi, M. Sohail, S. A. Joshi and J. Iqbal, *Int. J. Pharm.*, 2017, **533**, 125–137.
78 X. Z. Shu and K. J. Zhu, *Int. J. Pharm.*, 2002, **233**, 217–225.
79 S. Saravanan, S. Vimalraj, P. Thanikaivelan, S. Banudevi and G. Manivasagam, *Int. J. Biol. Macromol.*, 2019, **121**, 38–54.
80 H. Y. Zhou, L. J. Jiang, P. P. Cao, J. B. Li and X. G. Chen, *Carbohydr. Polym.*, 2015, **117**, 524–536.
81 A. Shi, X. Dai and Z. Jing, *Polym. Sci., Ser. A*, 2020, **62**, 228–239.
82 G. A. F. Roberts and K. E. Taylor, *Makro*, 1989, **190**, 951–960.
83 P. Hu, C. B. Raub, J. S. Choy and X. Luo, *J. Mater. Chem. B*, 2020, **8**, 2519–2529.
84 L. Gao, H. Gan, Z. Meng, R. Gu, Z. Wu, L. Zhang, X. Zhu, W. Sun, J. Li, Y. Zheng and G. Dou, *Colloids Surf., B*, 2014, **117**, 398–405.
85 R. A. Muzzarelli, M. El Mehtedi, C. Bottegoni, A. Aquili and A. Gigante, *Mar. Drugs*, 2015, **13**, 7314–7338.
86 G. Tripodo, A. Trapani, A. Rosato, C. Di Franco, R. Tamma, G. Trapani, D. Ribatti and D. Mandracchia, *Carbohydr. Polym.*, 2018, **198**, 124–130.
87 L. Pérez-Álvarez, L. Ruiz-Rubio, B. Artetxe, M. D. M. Vivanco, J. M. Gutiérrez-Zorrilla and J. L. Vilas-Vilela, *Carbohydr. Polym.*, 2019, **213**, 159–167.
88 L. Li, N. Wang, X. Jin, R. Deng, S. Nie, L. Sun, Q. Wu, Y. Wei and C. Gong, *Biomaterials*, 2014, **35**, 3903–3917.
89 E. A. Kamoun, *J. Adv. Res.*, 2016, **7**, 69–77.
90 E. Lucas de Lima, N. Fittipaldi Vasconcelos, J. da Silva Maciel, F. Karine Andrade, R. Silveira Vieira and J. P. Andrade Feitosa, *J. Mater. Sci.: Mater. Med.*, 2020, **31**, 5.
91 J. Berger, M. Reist, J. M. Mayer, O. Felt, N. A. Peppas and R. Gurny, *Eur. J. Pharm. Biopharm.*, 2004, **57**, 19–34.
92 L. Weng, X. Chen and W. Chen, *Biomacromolecules*, 2007, **8**, 1109–1115.
93 P. Sautrot-Ba, N. Razza, L. Breloy, S. A. Andaloussi, A. Chiappone, M. Sangermano, C. Hélary, S. Belbekhouche, T. Coradin and D. L. Versace, *J. Mater. Chem. B*, 2019, **7**, 6526–6538.
94 M. Pei, J. Mao, W. Xu, Y. Zhou and P. Xiao, *J. Polym. Sci., Part A: Polym. Chem.*, 2019, **57**, 1862–1871.
95 J. Huang, J. Qin, P. Zhang, X. Chen, X. You, F. Zhang, B. Zuo and M. Yao, *Carbohydr. Polym.*, 2020, **229**, 115515.
96 A. K. Ospanova, B. E. Savdenbekova, M. K. Iskakova, R. A. Omarova, R. N. Zhartybaev, B. Z. Nussip and A. S. Abdikadyr, *IOP Conf. Ser.: Mater. Sci. Eng.*, 2017, **230**, 1–6.
97 M. T. Cook, G. Tzortzis, V. V. Khutoryanskiy and D. Charalampopoulos, *J. Mater. Chem. B*, 2013, **1**, 52–60.
98 K. Tian, C. Xie and X. Xia, *Colloids Surf., B*, 2013, **109**, 82–89.
99 J. H. Bongaerts, J. J. Cooper-White and J. R. Stokes, *Biomacromolecules*, 2009, **10**, 1287–1294.
100 M. Criado-Gonzalez, M. Fernandez-Gutierrez, J. San Roman, C. Mijangos and R. Hernández, *Carbohydr. Polym.*, 2019, **206**, 428–434.

101 A. Ali and S. Ahmed, *Int. J. Biol. Macromol.*, 2018, **109**, 273–286.
102 L. Pérez-Álvarez, L. Ruiz-Rubio, I. Azua, V. Benito, A. Bilbao and J. L. Vilas-Vilela, *Eur. Polym. J.*, 2019, **112**, 31–37.
103 B. Guan, H. Wang, R. Xu, G. Zheng, J. Yang, Z. Liu, M. Cao, M. Wu, J. Song, N. Li, T. Li, Q. Cai, X. Yang, Y. Li and X. Zhang, *Sci. Rep.*, 2016, **6**, 1–12.
104 H. Lv, Z. Chen, X. Yang, L. Cen, X. Zhang and P. Gao, *J. Dent.*, 2014, **42**, 1464–1472.
105 S. Del Hoyo-Gallego, L. Pérez-Álvarez, F. Gómez-Galván, E. Lizundia, I. Kuritka, V. Sedlarik, J. M. Laza and J. L. Vila-Vilela, *Carbohydr. Polym.*, 2016, **143**, 35–43.
106 V. Nascimento, C. França, J. Hernández-Montelongo, D. Machado, M. Lancellotti, M. Cotta, R. Landers and M. Beppu, *Eur. Polym. J.*, 2018, **109**, 198–205.
107 L. Maddalena, F. Carosio, J. Gomez, G. Saracco and A. Fina, *Polym. Degrad. Stab.*, 2018, **152**, 1–9.
108 J. Jung, L. Li, C. K. Yeh, X. Ren and Y. Sun, *Mater. Sci. Eng., C*, 2019, **104**, 109961.
109 H. Wang, J. Qian and F. Ding, *J. Agric. Food Chem.*, 2018, **66**, 395–413.
110 S. Kumar, A. Mukherjee and J. Dutta, *Trends Food Sci. Technol.*, 2020, **97**, 196–209.
111 N. L. Benbow, J. L. Webber, S. Karpiniec, M. Krasowska, J. K. Ferri and D. A. Beattie, *Phys. Chem. Chem. Phys.*, 2017, **19**, 23790–23801.
112 T. I. Croll, A. J. O'Connor, G. W. Stevens and J. J. Cooper-White, *Biomacromolecules*, 2006, **7**, 1610–1622.
113 J. J. Richardson, M. Bjornmalm and F. Caruso, *Science*, 2015, **348**, aaa2491.
114 H. Kaygusuz, S. Micciulla, F. B. Erim and R. von Klitzing, *J. Polym. Sci., Part B: Polym. Phys.*, 2017, **55**, 1798–1803.
115 J. Huang, S. Zajforoushan Moghaddam and E. Thormann, *ACS Omega*, 2019, **4**, 2019–2029.
116 G. Decher, *Science*, 1997, **277**, 1232–1237.
117 J. B. Schlenoff, A. H. Rmaile and C. B. Bucur, *J. Am. Chem. Soc.*, 2008, **130**, 13589–13597.
118 R. V. Klitzing, *Phys. Chem. Chem. Phys.*, 2006, **8**, 5012.
119 D. Volodkin and R. von Klitzing, *Curr. Opin. Colloid Interface Sci.*, 2014, 1–7.
120 C. Coquery, F. Carosio, C. Negrell, N. Caussé, N. Pébère and G. David, *Surf. Interfaces*, 2019, **16**, 59–66.
121 W. Yuan, H. Dong, C. M. Li, X. Cui, L. Yu, Z. Lu and Q. Zhou, *Langmuir*, 2007, **23**, 13046–13052.
122 J. M. Silva, A. R. C. Duarte, S. G. Caridade, C. Picart, R. L. Reis and J. F. Mano, *Biomacromolecules*, 2014, **15**, 3817–3826.
123 G. Maurstad, Y. A. Mørch, A. R. Bausch and B. T. Stokke, *Carbohydr. Polym.*, 2008, **71**, 672–681.
124 P. Kujawa, P. Moraille, J. Sanchez, A. Badia and F. M. Winnik, *J. Am. Chem. Soc.*, 2005, **127**, 9224–9234.
125 T. Tariverdian, T. Navaei, P. B. Milan, A. Samadikuchaksaraei and M. Mozafari, in *Advanced Functional Polymers for Biomedical Applications*, ed. M. Mozafari and N. P. S. Chauhan, Elsevier, 2019, pp. 323–357.
126 J. A. Burdick and G. D. Prestwich, *Adv. Mater.*, 2011, **23**, 41–56.
127 H. H. Trimm and B. R. Jennings, *Biochem. J.*, 1983, **213**, 671–677.
128 N. Ghavidel Mehr, C. D. Hoemann and B. D. Favis, *Polymer*, 2015, **64**, 112–121.
129 J. Choi and M. F. Rubner, *Macromolecules*, 2005, **38**, 116–124.
130 M. Elzbieciak, S. Zapotoczny, P. Nowak, R. Krastev, M. Nowakowska and P. Warszyński, *Langmuir*, 2009, **25**, 3255–3259.
131 E. Guzmán, J. A. Cavallo, R. Chuliá-Jordán, C. Gómez, M. C. Strumia, F. Ortega and R. G. Rubio, *Langmuir*, 2011, **27**, 6836–6845.
132 C. Huang, G. Fang, Y. Zhao, S. Bhagia, X. Meng, Q. Yong and A. J. Ragauskas, *Carbohydr. Polym.*, 2019, **222**, 115036.
133 U. Voigt, V. Khrenov, K. Tauer, M. Hahn, W. Jaeger and R. V. Klitzing, *J. Phys.: Condens. Matter*, 2003, **15**, S213–S218.
134 S. Micciulla, S. Dodoo, C. Chevigny, A. Laschewsky and R. von Klitzing, *Phys. Chem. Chem. Phys.*, 2014, **16**, 21988–21998.
135 L. Richert, P. Lavalle, E. Payan, X. Z. Shu, G. D. Prestwich, J. F. Stoltz, P. Schaaf, J. C. Voegel and C. Picart, *Langmuir*, 2004, **20**, 448–458.
136 C. Picart, J. Mutterer, L. Richert, Y. Luo, G. D. Prestwich, P. Schaaf, J.-C. C. Voegel and P. Lavalle, *Proc. Natl. Acad. Sci. U. S. A.*, 2002, **99**, 12531–12535.
137 M. Zerball, A. Laschewsky and R. Von Klitzing, *J. Phys. Chem. B*, 2015, **119**, 11879–11886.
138 C. Liu, E. Thormann, P. M. Claesson and E. Tyrode, *Langmuir*, 2014, **30**, 8866–8877.
139 K. Wulf, S. Schünemann, A. Strohbach, R. Busch, S. B. Felix, K. P. Schmitz, K. Sternberg and S. Petersen, *BioNanoMaterials*, 2015, **16**, 265–273.
140 J. M. Silva, S. G. Caridade, N. M. Oliveira, R. L. Reis and J. F. Mano, *J. Mater. Chem. B*, 2015, **3**, 4555–4568.
141 N. M. Alves, C. Picart and J. F. Mano, *Macromol. Biosci.*, 2009, **9**, 776–785.
142 G. V. Martins, E. G. Merino, J. F. Mano and N. M. Alves, *Macromol. Biosci.*, 2010, **10**, 1444–1455.
143 A. F. Martins, J. Vlcek, T. Wigmosta, M. Hedayati, M. M. Reynolds, K. C. Popat and M. J. Kipper, *Appl. Surf. Sci.*, 2020, **502**, 144282.
144 M. Marudova, S. Lang, G. J. Brownsey and S. G. Ring, *Carbohydr. Res.*, 2005, **340**, 2144–2149.
145 A. E. Sorkio, E. P. Vuorimaa-Laukkanen, H. M. Hakola, H. Liang, T. A. Ujula, J. J. Valle-Delgado, M. Österberg, M. L. Yliperttula and H. Skottman, *Biomaterials*, 2015, **51**, 257–269.
146 M. Andonegi, K. L. Heras, E. Santos-Vizcaíno, M. Igartua, R. M. Hernandez, K. de la Caba and P. Guerrero, *Carbohydr. Polym.*, 2020, **237**, 116159.
147 I. Leceta, P. Arana, P. Guerrero and K. De La Caba, *Mater. Lett.*, 2014, **128**, 125–127.
148 A. Sionkowska and A. Płanecka, *J. Mol. Liq.*, 2013, **186**, 157–162.
149 T. Yovcheva, B. Pilicheva, A. Marinova, A. Viraneva, I. Bodurov, G. Exner, S. Sotirov, I. Vlaeva, Y. Uzunova and M. Marudova, *J. Phys.: Conf. Ser.*, 2019, **1186**, 1–7.

150 K. Junka, O. Sundman, J. Salmi, M. Österberg and J. Laine, *Carbohydr. Polym.*, 2014, **108**, 34–40.
151 K. Cai, Y. Hu, Y. Wang and L. Yang, *J. Biomed. Mater. Res.*, 2008, **84A**, 516–522.
152 A. Dedinaite, M. Lundin, L. Macakova and T. Auletta, *Langmuir*, 2005, **21**, 9502–9509.
153 H. Huang and X. Yang, *Colloids Surf., A*, 2003, **226**, 77–86.
154 A. Valverde, L. Pérez-Álvarez, L. Ruiz-Rubio, M. A. Pacha Olivenza, M. B. García Blanco, M. Díaz-Fuentes and J. L. Vilas-Vilela, *Carbohydr. Polym.*, 2019, **207**, 824–833.
155 H. Zare, G. D. Najafpour, M. Jahanshahi, M. Rahimnejad and M. Rezvani, *Rom. Biotechnol. Lett.*, 2017, **22**, 12611–12619.
156 H. Sun, D. Choi, J. Heo, S. Y. Jung and J. Hong, *Cancers*, 2020, **12**, 1–14.
157 P. Li, Y.-N. Dai, J.-P. Zhang, A.-Q. Wang and Q. Wei, *Int. J. Biomed. Sci.*, 2008, **4**, 221–228.
158 I. M. Brasil, C. Gomes, A. Puerta-Gomez, M. E. Castell-Perez and R. G. Moreira, *LWT–Food Sci. Technol.*, 2012, **47**, 39–45.
159 Y. Kusumastuti, A. Istiani, Rochmadi and C. W. Purnomo, *Adv. Mater. Sci. Eng.*, 2019, **2019**, 1–8.
160 J. B. Schlenoff, S. T. Dubas and T. Farhat, *Langmuir*, 2000, **16**, 9968–9969.
161 K. C. Krogman, N. S. Zacharia, S. Schroeder and P. T. Hammond, *Langmuir*, 2007, **23**, 3137–3141.
162 K. C. Krogman, J. l. Lowery, N. S. Zacharia, G. C. Rutledge and P. T. Hammond, *Nat. Mater.*, 2009, **8**, 512–518.
163 A. Izquierdo, S. S. Ono, J.-C. C. Voegel, P. Schaaf and G. Decher, *Langmuir*, 2005, **21**, 7558–7567.
164 M. Kolasinska, R. Krastev, T. Gutberlet and P. Warszynski, *Langmuir*, 2009, **25**, 1224–1232.
165 M. Criado, E. Rebollar, A. Nogales, T. A. Ezquerra, F. Boulmedais, C. Mijangos and R. Hernández, *Biomacromolecules*, 2017, **18**, 169–177.
166 M. Bulwan, S. Zapotoczny and M. Nowakowska, *Soft Matter*, 2009, **5**, 4726–4732.
167 I. Langmuir, *J. Am. Chem. Soc.*, 1917, **39**, 1848–1906.
168 K. B. Blodgett, *J. Am. Chem. Soc.*, 1935, **57**, 1007–1022.
169 F. J. Pavinatto, L. Caseli and O. N. Oliveira, *Biomacromolecules*, 2010, **11**, 1897–1908.
170 P. T. Hammond, *Adv. Mater.*, 2004, **16**, 1271–1293.
171 Y. Sakai-Otsuka, S. Zaioncz, I. Otsuka, S. Halila, P. Rannou and R. Borsali, *Macromolecules*, 2017, **50**, 3365–3376.
172 Y. Liao, W.-C. Chen and R. Borsali, *Adv. Mater.*, 2017, **29**, 1701645.
173 N. Ayres, *Polym. Chem.*, 2010, **1**, 769–777.
174 O. Azzaroni, *J. Polym. Sci., Part A: Polym. Chem.*, 2012, **50**, 3225–3258.
175 H. S. Lee, D. M. Eckmann, D. Lee, N. J. Hickok and R. J. Composto, *Langmuir*, 2011, **27**, 12458–12465.
176 H. S. Lee, M. Q. Yee, Y. Y. Eckmann, N. J. Hickok, D. M. Eckmann and R. J. Composto, *J. Mater. Chem.*, 2012, **22**, 19605–19616.
177 P. Kurt, L. Wood, D. E. Ohman and K. J. Wynne, *Langmuir*, 2007, **23**, 4719–4723.
178 N. Gorochovceva, A. Naderi, A. Dedinaite and R. Makuška, *Eur. Polym. J.*, 2005, **41**, 2653–2662.
179 Y. Zhou, B. Liedberg, N. Gorochovceva, R. Makuska, A. Dedinaite and P. M. Claesson, *J. Colloid Interface Sci.*, 2007, **305**, 62–71.
180 M. Xie, K. Huang, F. Yang, R. Wang, L. Han, H. Yu, Z. Ye and F. Wu, *Int. J. Biol. Macromol.*, 2020, **151**, 1116–1125.
181 S. Velmurugan, S. Palanisamy, T. C.-K. Yang, M. Gochoo and S.-W. W. Chen, *Ultrason. Sonochem.*, 2020, **62**, 104863.
182 L. Lisuzzo, G. Cavallaro, F. Parisi, S. Milioto, R. Fakhrullin and G. Lazzara, *Coatings*, 2019, **9**, 70.
183 M. Koosha and S. Hamedi, *Prog. Org. Coat.*, 2019, **127**, 338–347.
184 F. I. Ali, S. T. Mahmoud, F. Awwad, Y. E. Greish and A. F. Abu-Hani, *Carbohydr. Polym.*, 2020, **236**, 116064.
185 A. Giannakas, P. Stathopoulou, G. Tsiamis and C. Salmas, *J. Food Process. Preserv.*, 2020, **44**, e14327.
186 V. Labonté, A. Marion, N. Virgilio and J. R. Tavares, *Ind. Eng. Chem. Res.*, 2016, **55**, 7362–7372.
187 M. H. Mostafa, M. A. Elsawy, M. S. Darwish, L. I. Hussein and A. H. Abdaleem, *Mater. Chem. Phys.*, 2020, **248**, 122914.
188 Q. Peng, M. Liu, J. Zheng and C. Zhou, *Microporous Mesoporous Mater.*, 2015, **201**, 190–201.
189 G. Cavallaro, S. Milioto, L. Nigamatzyanova, F. Akhatova, R. Fakhrullin and G. Lazzara, *ACS Appl. Nano Mater.*, 2019, **2**, 3169–3176.
190 G. Cavallaro, S. Milioto and G. Lazzara, *Langmuir*, 2020, **36**, 3677–3689.
191 G. Cavallaro, G. Lazzara, S. Konnova, R. Fakhrullin and Y. Lvov, *Green Mater.*, 2014, **2**, 232–242.
192 H. Pan, W. Wang, Y. Pan, L. Song, Y. Hu and K. M. Liew, *Carbohydr. Polym.*, 2015, **115**, 516–524.
193 M. Hassan, M. Nour, Y. Abdelmonem, G. Makhlouf and A. Abdelkhalik, *Polym. Degrad. Stab.*, 2016, **133**, 8–15.
194 B.-I. Andreica, X. Cheng and L. Marin, *Eur. Polym. J.*, 2020, **139**, 110016.
195 L. J. R. Foster, S. Ho, J. Hook, M. Basuki and H. Marçal, *PLoS One*, 2015, **10**, e0135153.
196 G. Cavallaro, G. Lazzara, S. Konnova, R. Fakhrullin and Y. Lvov, *Green Mater.*, 2014, **2**, 232–242.
197 V. Bertolino, G. Cavallaro, G. Lazzara, S. Milioto and F. Parisi, *New J. Chem.*, 2018, **42**, 8384–8390.
198 T. C. Yadav, P. Saxena, A. K. Srivastava, A. K. Singh, R. K. Yadav, Harish, R. Prasad and V. Pruthi, *Advanced Functional Textiles and Polymers*, Wiley, 2019, pp. 365–403.
199 M. Rubina, A. Shulenina, R. Svetogorov and A. Vasilkov, *Macromol. Symp.*, 2020, **389**, 1900067.
200 R. Ying, H. Wang, R. Sun and K. Chen, *Mater. Sci. Eng., C*, 2020, **110**, 110689.
201 X. Jia, I. Ahmad, R. Yang and C. Wang, *J. Mater. Chem. B*, 2017, **5**, 2459–2467.
202 A. B. Neji, M. Jridi, H. Kchaou, M. Nasri and R. Dhouib Sahnoun, *Polym. Test.*, 2020, **84**, 106380.
203 V. Bertolino, G. Cavallaro, G. Lazzara, M. Merli, S. Milioto, F. Parisi and L. Sciascia, *Ind. Eng. Chem. Res.*, 2016, **55**, 7373–7380.
204 M. Liu, Y. Zhang, C. Wu, S. Xiong and C. Zhou, *Int. J. Biol. Macromol.*, 2012, **51**, 566–575.
205 L. Lisuzzo, G. Cavallaro, S. Milioto and G. Lazzara, *New J. Chem.*, 2019, **43**, 10887–10893.

206 M. Liu, C. Wu, Y. Jiao, S. Xiong and C. Zhou, *J. Mater. Chem. B*, 2013, **1**, 2078.
207 I. Benucci, K. Liburdi, I. Cacciotti, C. Lombardelli, M. Zappino, F. Nanni and M. Esti, *Food Hydrocolloids*, 2018, **74**, 124–131.
208 X. Liu, S. Qin, H. Li, J. Sun, X. Gu, S. Zhang and J. C. Grunlan, *Macromol. Mater. Eng.*, 2019, **304**, 1800531.
209 J. Prakash, D. Prema, K. Venkataprasanna, K. Balagangadharan, N. Selvamurugan and G. D. Venkatasubbu, *Int. J. Biol. Macromol.*, 2020, **154**, 62–71.
210 X. Li, Y.-C. Li, M. Chen, Q. Shi, R. Sun and X. Wang, *J. Mater. Chem. B*, 2018, **6**, 6544–6549.
211 Z.-K. Cui, S. Kim, J. J. Baljon, B. M. Wu, T. Aghaloo and M. Lee, *Nat. Commun.*, 2019, **10**, 3523.